Echo Cancellation and Equalization for Primary Rate ISDN Service in the Subscriber Loop Plant

by

Srikanth Subramanian
B.E, Anna University, 1991

A Thesis Submitted in Partial Fulfillment of the
Requirements for the Degree of

M.A.Sc

in the Department of
Electrical and Computer Engineering

We accept this thesis as conforming
to the required standard

[redacted]
Dr. D. J. Shpak, Co-Supervisor

[redacted]
Dr. A. Antoniou, Co-Supervisor

[redacted]
Dr. G. McLean, Outside Member

[redacted]
Dr. S. Waddell, External Examiner

Supervisors: Dr. D. J. Shpak and Dr. A. Antoniou

ABSTRACT

The main objective of this work is to study echo cancellation and equalization for primary rate ISDN service in the subscriber loop plant. Such a system will enable T1-rate services over the subscriber loop by using transceivers at either end of the telephone connection.

Echo cancellation and equalization are two important functions needed in the transceiver for achieving the high communication rate over unconditioned subscriber lines. These functions use adaptive filtering concepts and form the main focus of our research.

Duplex communication over the subscriber loop plant is achieved by using echo cancellation. We use simulation models to demonstrate a successful echo canceler for worst-case conditions. The echo canceler satisfies preset performance conditions. Some techniques for reducing the length of the echo canceler are also presented along with successful simulation results.

Equalization is primarily used for eliminating interference from different signals in the same multipair cable. A recently developed theory is used to achieve a successful equalization strategy for this primary rate service. A simulation environment built for the equalizer is detailed and satisfactory equalizer performance is shown to be achieved using extensive simulation results.

Examiners:

[redacted]

Dr. D. J. Shpak, Co-Supervisor

[redacted]

Dr. A. Antoniou, Co-Supervisor

[redacted]

Dr. G. McLean, Outside Member

[redacted]

Dr. S. Waddell, External Examiner

Table of Contents

List of Figures

List of Tables

Acknowledgments

I wish to express my gratitude to my supervisors, Dr. D. J. Shpak and Dr. A. Antoniou of the Department of Electrical and Computer Engineering for their encouragement, guidance, and advice during the course of this work and for their help in preparation of the thesis.

I would also like to express my thanks to Dr. P. S. R. Diniz for his patient support and guidance during his stay at the University of Victoria and later on through e-mail. His help in the preparation of this thesis is also acknowledged.

Financial assistance received from Dr. D. J. Shpak and Dr. A. Antoniou through Micronet, National Centres of Excellence Program, is gratefully acknowledged.

I would like to thank Dr. D. Falconer at Carleton University for helping me to get in touch with his students and sending me some of his publications. I would also like to thank M. Abdulrahman at Carleton University and B. R. Petersen at IBM, Zurich for answering many of my doubts and sending valuable code and data for understanding some of their research contributions.

Thanks are due to B. Gerson at Pacific Microelectronics Center for bringing the problem to our notice and his help in sending us many related publications.

Thanks are also due to W. A. Keddy for answering so many questions regarding the word processing package used in the preparation of this document. I would also like to express my thanks to R. Kelly for his computer support during the course of my stay here.

Finally, I would like to thank my parents and the *gang* in the Victoria Micronet Centre for their support throughout my stay here. All of them made this thesis a very rewarding experience.

List of Abbreviations

2B1Q	2-binary-to-1-quarternary
3B2T	3-binary-to-2-ternary
AIFIR	Adaptive interpolated FIR filter
CSA	Carrier-serving area
DDE	Decision-directed equalizer
DFE	Decision-feedback equalizer
DSL	Digital subscriber line
FRLS	Fast recursive least squares
FEXT	Far-end crosstalk
FIR	Finite-duration impulse response
FSE	Fractionally-spaced equalizer
HDSL	High bit-rate digital subscriber line
IFFT	Inverse fast Fourier transform
ISDN	Integrated services digital network
ISI	Intersymbol interference
MSE	Mean-squared error
MMSE	Minimum mean-squared error
NEXT	Near-end crosstalk
PCM	Pulse code modulation
RLS	Recursive least squares
LMS	Least-mean squares

SSE	Symbol-spaced equalizer
T	Sampling period
TCM	Time compression multiplexing

Chapter 1

Introduction

1.1 Introduction

The world-wide subscriber loop plant for telephone service has grown enormously to encompass billions of miles of copper wires. This copper plant remains one of the world's greatest and most valued technological assets. Although it is hoped that fiber-in-the-loop installation will bring widespread broadband applications to residential customers by the end of this decade, there is an urgent need to explore new technologies for immediate applications which meet the growing wideband service needs of the customer. While an evolution to optical fiber seems inevitable, the existing investment in copper wire ensures that wire will still be an important communications medium during the transition to optical fiber over the next few decades. The telecommunications industry, eager to extend the useful lifetime of the existing copper plant and at the same time provide high-speed digital services, has a keen interest in the development and implementation of technologies that allow low-cost high-speed services over the copper loop plant [1].

One existing wideband service is the T1 service normally used by businesses for voice multiplexing and digital data transmission. The T1 service transmits a uni-directional pulse code modulated signal (PCM) signal at a 1.544 Mbits/s rate over a wire pair (simplex method). Two pairs are required for this bidirectional service, which is used mainly along trunk routes where cable lengths are long. To overcome the signal loss resulting from attenuation in the long cables, repeater sections are needed for every 6000 ft of 22-gauge cable. Moreover, bridged taps must be removed in the lines and pair selection is needed to be done in some cases. These engineering requirements of the T1 service, which are clearly outlined in [2], can result in long lead times for the installation of

T1 service and can be expensive.

The recently proposed high bit-rate digital subscriber line (HDSL) scheme will enable T1-rate service over existing unconditioned, repeaterless subscriber lines, thereby circumventing the problems mentioned above. The objective of this scheme is to avoid the time and expense associated with pair selection, bridged tap removal and repeater installation required for conventional T1 service. In the HDSL system, these procedures are eliminated by improving the line transceivers, the performance of which forms the main focus of our work.

If classical fixed filters were used in the transceiver, considerable engineering and customization would be required to accommodate the wide range of loop characteristics encountered in the distribution plant. The advent of adaptive filtering techniques and VLSI technology have made feasible cost- and space-effective circuitry that will enable high bit-rate services over existing lines.

Adaptive filtering techniques have been successfully applied to providing basic rate (160 Kbits/s) digital subscriber line (DSL) services in the loop plant and serve as a starting point for HDSL technologies. The DSL technology has enabled telephone companies to assign integrated services digital network (ISDN) basic access service in a ubiquitous non-engineered fashion, similar to the way conventional voice service is provided. HDSL is expected to be a transitional technology supporting primary rate ISDN (1.544 Mbits/s) service in the subscriber loop while providing a smooth transition towards fiber-based services [3]. There is considerable incentive to develop and deploy HDSL technology quickly since telephone companies want to shorten service-provisioning intervals to customers while more economically providing T1-rate services.

1.2 The HDSL System

The HDSL system uses two twisted-pair carrier-serving area (CSA) loops [3] as illustrated in Fig. 1.1. CSA is a plant administration area surrounding a wire centre or a remote terminal. Loops within a CSA that do not include any 26-gauge cable pairs are restricted to lengths of 12 kft including any bridged-tap length. If 26-gauge pairs are used anywhere in the loop, the total length is restricted to 9 kft with no single bridged tap longer than 2 kft. CSA is a reasonably standard operation and planning concept in most of the telephone operating areas in North America. In the HDSL sys-

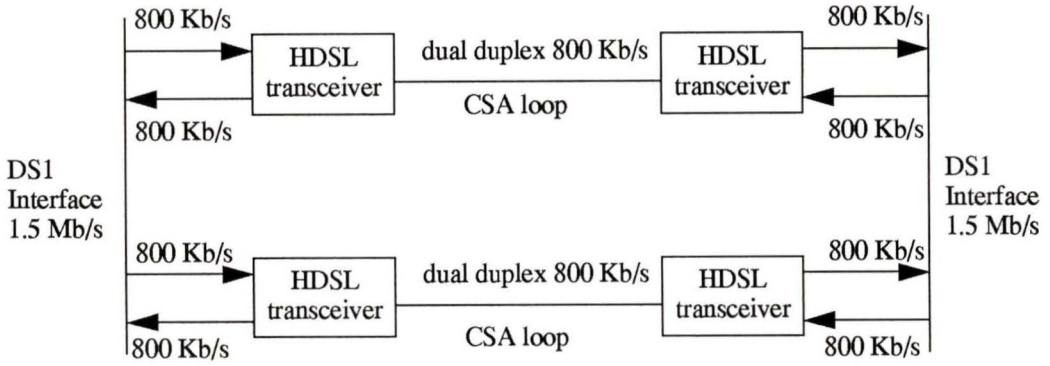

Figure 1.1 HDSL dual duplex scheme

tem, unlike the dual-simplex T1 service, each pair has a bidirectional data rate of 800 Kbits/s to deliver T1-rate service using full-duplex transmission. The most important aspect of the HDSL system is the use of high performance transceivers to overcome the deficiencies resulting from using low-grade unconditioned subscriber lines when providing high-speed duplex service. The individual elements of the HDSL transceiver are shown in Fig. 1.2 and will be described in more detail.

The scrambler, which randomizes the input bit sequence, reduces sequence correlation and improves the convergence of the adaptive filters. It also provides a sequence rich in timing information since, for example, it reduces the possibility of long sequences of zeros that have no timing information. The line coder can be viewed as a modulation scheme for baseband transmission. Line codes are often selected to serve multiple requirements which may include reducing near-end crosstalk (NEXT) disturbance; reducing the symbol rate by using multi-level codes; aiding echo cancellation, equalization, and timing recovery; reduction of sensitivity to inaccuracy in the transmit and receive filters [4][5]. One should not lose sight of any of these concerns since the ultimate goal is to achieve as error-free transmission as possible. The prescribed error rate requirement for the HDSL system is 10^{-7}. Block codes like 2-binary-to-1-quarternary (2B1Q), 3-binary-to-2-ternary (3B2T) are useful in reducing the symbol rate in the system since each symbol contains more than one bit of information. The four level 2B1Q code has been chosen as the line code standard in North America due to the overall better performance achieved in comparison with other line codes [3][5]. Since two bits are encoded into each 2B1Q symbol, this line code reduces the symbol rate to 400 Ksymbols/s. Because the chan-

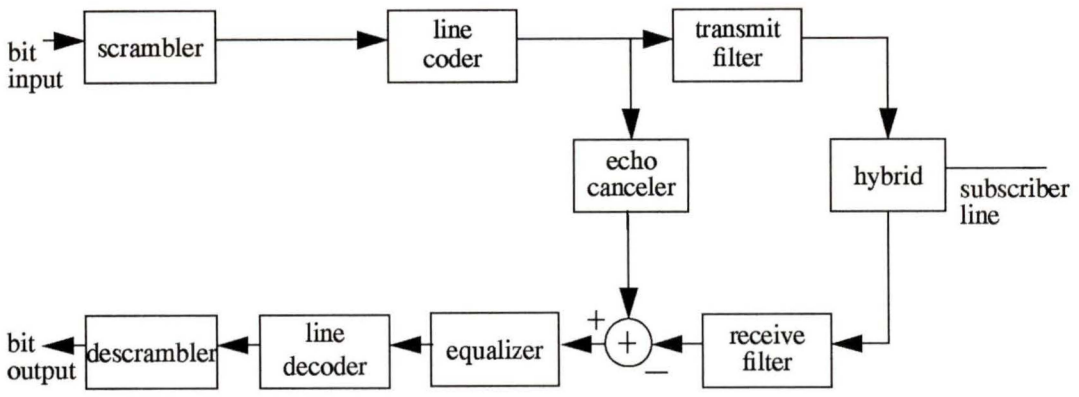

Figure 1.2 HDSL transceiver block diagram

nel greatly attenuates high frequencies, this lower frequency reduces the attenuation due to the channel and thus increases the system reach (maximum transmission distance). Also, code 2B1Q reduces the rate at which hardware is required to operate. Notably, the performance of 2B1Q has been found to be very good in the DSL environment [3]. The advantage of using such a block code becomes more evident when NEXT is considered.

Near-end crosstalk is a major obstacle facing HDSL system designers. It is caused by the coupling of similar HDSL signals in the same multi-pair cable. Typically, in a cable there may be 49 other similar lines carrying HDSL signals. All these transmitters could contribute towards crosstalk, where the signal coupling increases with frequency [6]. Since a reduction in high frequency content contributes toward reducing the NEXT interference in the loop plant, line coding schemes like 2B1Q, which effectively halve the signal bandwidth, are beneficial.

The transmit filter is used for pulse shaping and band-limits the signal by removing high-frequency components from the sharp rise and fall times of the 2B1Q signal. A similar filter on the receiver side is used to suppress high-frequency noise and also acts as an anti-aliasing filter before analog-to-digital conversion. The duplex transmission scheme used in the HDSL system necessitates the use of a hybrid which separates the signal in the two directions. The hybrid is essentially an impedance bridge that is used to match the input impedance of the line at all frequencies of interest thus reducing the leakage of the near-end transmit signal into the receiver. The non-idealities in the hybrid circuit (detailed later) result in an undesir-

able attenuated copy, or echo, of the near-end transmit signal which appears at the receiver input along with the far-end signal. This echo can be overcome in two ways: using either time compression multiplexing (TCM) or echo cancellation. In TCM, transmission from each end of the line is interleaved such that there is only one active signal in the channel at any given time and therefore near-end echoes and NEXT are avoided [5]. Echoes are avoided as the transmission is effectively simplex in nature and bursts of data are sent in either direction with time separation for delay.

The NEXT is avoided by synchronizing the transmitters at the central office where there is more chance of NEXT occurring. Synchronization means that all transmitters are active for a particular time period and receive during a particular period without any overlap between these functions; hence the NEXT can be avoided. The disadvantage with this scheme is that it effectively doubles the required signal bandwidth (nearly 2.25 times after compensating for the delay) thereby increasing both the attenuation and dispersion which results in reduced system reach. The TCM transmission method is very popular in Japan [7]. In the echo cancellation method, a copy of the transmit sequence is input to an adaptive filter (echo canceler) which is used to model the echo path comprising the hybrid and the transmit and receive filters. This method was chosen over the TCM in DSL implementation and is also the accepted standard for the HDSL system in North America [5].

The subscriber loop plant to be used for HDSL service was originally designed for low frequency (< 10 kHz) voice signals and signals much higher in frequency than this are subjected to attenuation and phase distortion. In the HDSL system, this results in symbols being widely dispersed while travelling down the line and thereby interfering with adjacent symbols at the receiver. This source of interference which is known as intersymbol interference (ISI), is quite significant owing to the short symbol spacing (2.5 microseconds) and each dispersed pulse can interfere with hundreds of other symbols. An adaptive decision-feedback equalizer (DFE), which uses previously detected symbols, is the best solution for suppressing ISI without significant noise enhancement [8][9].

1.3 Thesis Organization

Our main motivation in this work is to study the performance of echo cancelers and equalizers for the HDSL system. These two elements in an HDSL transceiver use adaptive filtering concepts and this is the main focus of our research. A brief introduction to the HDSL system has been given in Sec. 1.2.

The echo canceler has to meet certain performance standards and these are outlined in chapter 2. A major concern of many vendors is the length of the echo canceler needed to operate satisfactorily and possible reductions in complexity for achieving the same performance. Another issue is the interfacing of the echo canceler with an equalizer in a transceiver. These issues are covered in the chapter 2.

The NEXT along with ISI is an important impediment that needs to be overcome for reliable transmission of data. The working of an adaptive equalizer to overcome the above problems is explained in the chapter 3. A complete simulation environment which exploits certain NEXT conditions is used to demonstrate the working of an adaptive equalizer satisfactorily.

Conclusions from the work are presented in the chapter 4 along with suggestions for further work.

Chapter 2

HDSL Echo Cancellation

2.1 Introduction

The HDSL system uses a dual duplex scheme to achieve the required bit rate over the subscriber loop. Duplex communication necessitates separation of signals transmitted in either direction at the transceivers. Echoes are signals from a transmitter which reach the same or *near-end* receiver due to various reasons [10]. Typically, hybrids are used at each transceiver for reducing the transmit signal leakage into the near-end receiver [11].

Echoes which arise in voice communications are different from those caused in data communication [10] as voice echoes are mainly influenced by the round-trip delays in the connection [11]. In HDSL, the main source of echo is the leakage of the transmit signal to the receiver through the hybrid. A hybrid is a circuit which is used to couple the transmit signal (in a simplex line) into the duplex line with minimal possible leakage into the near-end receiver. In effect, a hybrid is used to match the input impedance of the line to which it is connected. Due to the diverse nature of loops in the subscriber loop plant it is impossible to arrive at a hybrid circuit which will provide an exact match with every line used for providing HDSL service. A reasonable solution under these circumstances is to use a compromise circuit which provides a reasonable match over the range of lines in the loop plant. This, of course, results in near-end echoes due to the impedance mismatch at the hybrid. Even a small echo power is significant in HDSL due to the high attenuation suffered by the far-end signal. As a consequence, detection of the far-end symbol sequence could be greatly affected by this echo.

Impedance mismatch between the line and the hybrid, which causes the echo, is worsened by bridged taps, gauge mixing, and imperfect termination. All the HDSL loops have to satisfy the CSA criterion which restricts the maximum number of bridged

taps in a loop to two [12]. As a result, bridged taps have comparatively restricted influence on the echo. Bridged taps are usually found near the customer end since lines are branched out near the customer in anticipation of future customers or service [12]. Hence the effect of bridged taps is more dominant in the customer side echo, and this will be evident in the later sections.

The CSA loops are restricted to 24- and 26-gauge wires and the echo power caused due to gauge mixing is insignificant. The echoes due to imperfect termination at the far end suffer more loss than the signal and are also insignificant.

In this chapter, we shall study some worst-case echo paths for CSA loops from both the central office and the customer sides. The modeling of these echo paths will be outlined and the echo paths simulated using this modeling procedure will be illustrated. One of the main concerns of HDSL system vendors is the order of the echo-canceler needed for achieving satisfactory performance. This forms one of the main issues in this work and the order of the canceler working successfully in a HDSL context is obtained using calculations and simulations. Two techniques for reducing the order of the echo canceler are presented and two other echo-cancellation techniques proposed in the literature are investigated for HDSL echo cancellation. The simulation environment for this work was built using MATLAB^{TM}.

2.2 Echo-Path Modeling

The main challenge in HDSL echo cancellation results from the fact that the far-end signal which is to be detected by the transceiver suffers high loss due to the subscriber loop loss characteristics, which are significant at the HDSL transmission rates. Typically, the echo power at the receiver input could be 25-30 dB above the attenuated far-end signal and the relative power levels of the signal, echo, crosstalk, and white noise will be illustrated in the next chapter. As a consequence, the echo power has to be made small enough so that it does not form a major source of interference in the detection of the far-end signal. Previous studies of the loop plant have shown the need for a 60 dB echo cancellation level [13], and this figure includes the margins for finite precision and other effects which might not be included in a computer simulation model. Our main goal in this work is to achieve a 60 dB echo cancellation level using various techniques.

The first task toward this goal is to obtain a good model for HDSL echo paths

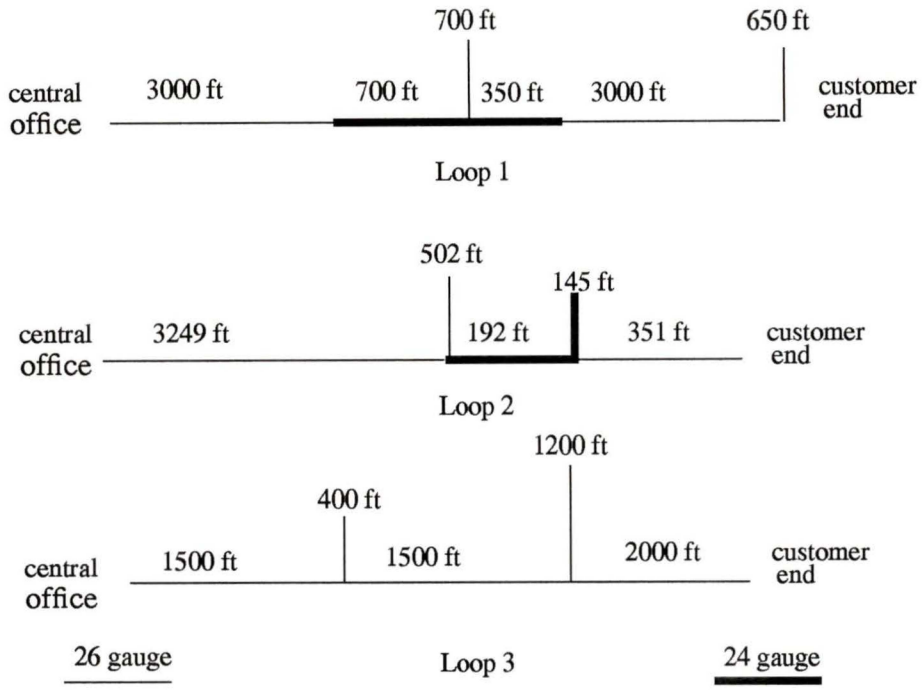

Figure 2.1 CSA test loops for echo cancellation

from standard CSA loop configurations and a hybrid model. In our study, we consider three worst-case loops with two bridged taps each for testing the performance of the echo cancelers. Both the customer-end and the central office echo paths will be investigated. The loops used in this study are shown in Fig. 2.1 and were obtained from [13][14][15].

The hybrid model and the transformer used in our echo-path modeling are shown in Figs. 2.2 and 2.3 respectively. They were obtained from [16]. The echo-path transfer function is given by

$$H(s) = \frac{Z_{bal}}{Z_o + Z_{bal}} - \frac{Z_{in}}{Z_o + Z_{in}} \tag{2.1}$$

where Z_{bal} is the balance impedance (110 ohms), Z_{in} is the input impedance of the loop looking in through the transformer, and Z_o is the series impedance of the hybrid.

The input impedance of the line is calculated using frequency dependent *ABCD*

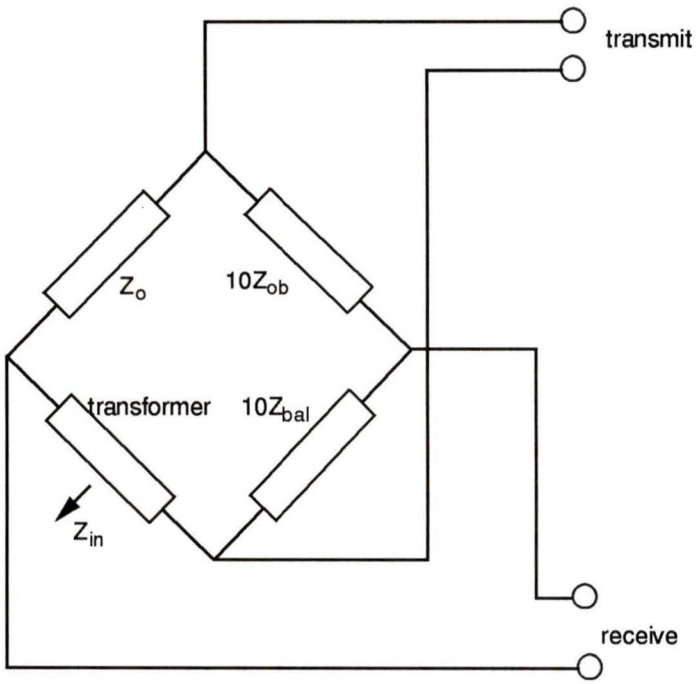

Figure 2.2 Hybrid equivalent circuit

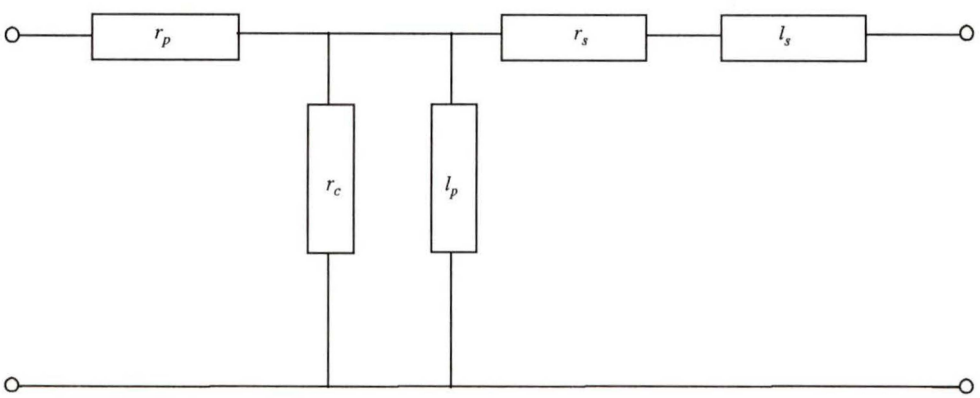

l_s = 0.002 mH
r_c = 10 kohms
l_p = 3 mH
r_p = 0.85 ohms
r_s = 0.85 ohms

Figure 2.3 Transformer model

parameters [16]. These parameters are obtained using the propagation constants [6] of the specific gauge cable which were obtained from [17]. The line can be made up of different sections involving gauge mixing and bridged taps. The use of the *ABCD* parameters is convenient because each section of the cable can be represented by its own parameters and the cascade of these is used to obtain the *ABCD* representation for the entire cable. For Loop 1 we obtain

$$\begin{bmatrix} A & B \\ C & D \end{bmatrix} = \begin{bmatrix} A_1 & B_1 \\ C_1 & D_1 \end{bmatrix} \begin{bmatrix} A_2 & B_2 \\ C_2 & D_2 \end{bmatrix} \begin{bmatrix} A_{br1} & B_{br1} \\ C_{br1} & D_{br1} \end{bmatrix} \begin{bmatrix} A_3 & B_3 \\ C_3 & D_3 \end{bmatrix} \begin{bmatrix} A_4 & B_4 \\ C_4 & D_4 \end{bmatrix} \begin{bmatrix} A_{br2} & B_{br2} \\ C_{br2} & D_{br2} \end{bmatrix} \tag{2.2}$$

where the parameters with numbered suffixes represent the different sections of the line and the parameters with suffixes *br1* and *br2* represent the parameters for the bridged tap sections in the cable. The transformers at either end of the line are used for coupling the signals to the line and to provide DC isolation. The *ABCD* parameters of the transformer are calculated as

$$A_{tr} = (Z_1 + Z_3)/ Z_3$$

$$B_{tr} = (Z_1Z_2 + Z_2Z_3 + Z_1Z_3)/ Z_3$$

$$C_{tr} = 1/ Z_3$$

$$D_{tr} = (Z_2 + Z_3)/ Z_3$$

where

$$Z_1 = r_p$$

$$Z_2 = r_s + j\omega ls$$

$$Z_3 = r_c \parallel j\omega l_p$$

and the values of the transformer model components r_p, r_c, l_l, l_p are given in Fig. 2.3. Using the above formula, the transformer *ABCD* parameters are calculated and are combined with the line's parameters as

$$\begin{bmatrix} A_l & B_l \\ C_l & D_l \end{bmatrix} = \begin{bmatrix} A_{tr} & B_{tr} \\ C_{tr} & D_{tr} \end{bmatrix} \begin{bmatrix} A & B \\ C & D \end{bmatrix} \begin{bmatrix} A_{tr} & B_{tr} \\ C_{tr} & D_{tr} \end{bmatrix} \tag{2.3}$$

where A_l, B_l, C_l, D_l are the *ABCD* parameters of the cable with the transformers at either end. Thus a complete *ABCD* description of the cable along with bridged taps, gauge mixing, and line transformers is obtained. Using this *ABCD* matrix, the input impedance of the line can be calculated as

$$Z_{in} = \frac{A_l + \frac{B_l}{Z_l}}{C_l + \frac{D_l}{Z_l}} \tag{2.4}$$

where Z_l is the load impedance (110 ohms). This can be used in estimating the frequency response of the echo path using (2.1).

In our simulation model, the *ABCD* parameters were calculated from DC to 6400 kHz (16 times the symbol rate). The inverse fast Fourier transform (IFFT) is used to obtain a time-domain echo-path model (echo-path impulse response) sampled at a very high rate. The reason for sampling the echo-path response at these high frequencies (compared to the symbol-rate) is for observing the effect of sampling phase on the echo cancelers and for possible future work in combining fractionally-spaced equalizers with echo cancelers in a HDSL transceiver [18]. A decimator is used to obtain echo-path impulse responses sampled at lower sampling rates. The different echo paths obtained using this method for the three loops in Fig. 2.1 for both the central office and the customer ends are shown in Figs. 2.4 and 2.5, respectively.

2.3 Order of the HDSL Echo Canceler

One of the main objectives of this work is to estimate the required order of the echo canceler needed to achieve the necessary cancellation level of 60 dB. A theoretical estimate of the echo canceler order needed for the above purpose is obtained from [13] as

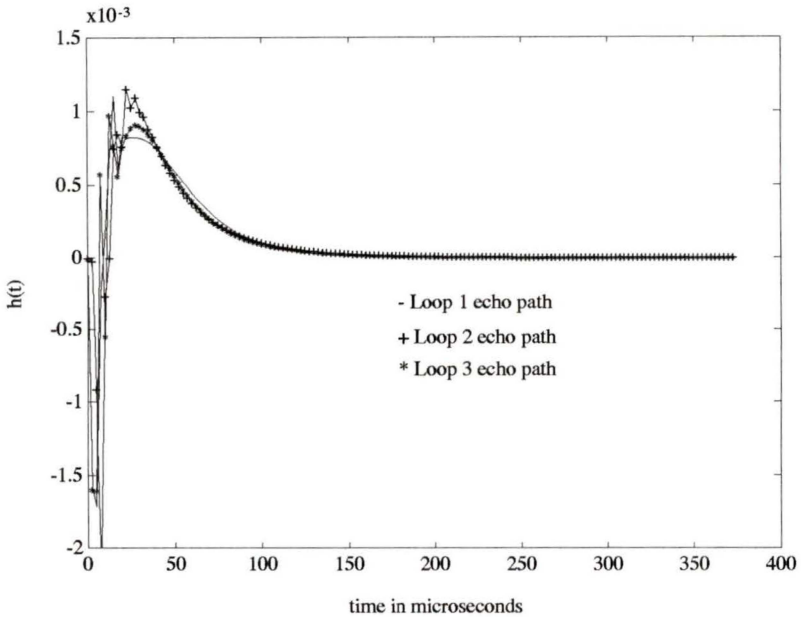

Figure 2.4 Central office echo path impulse responses

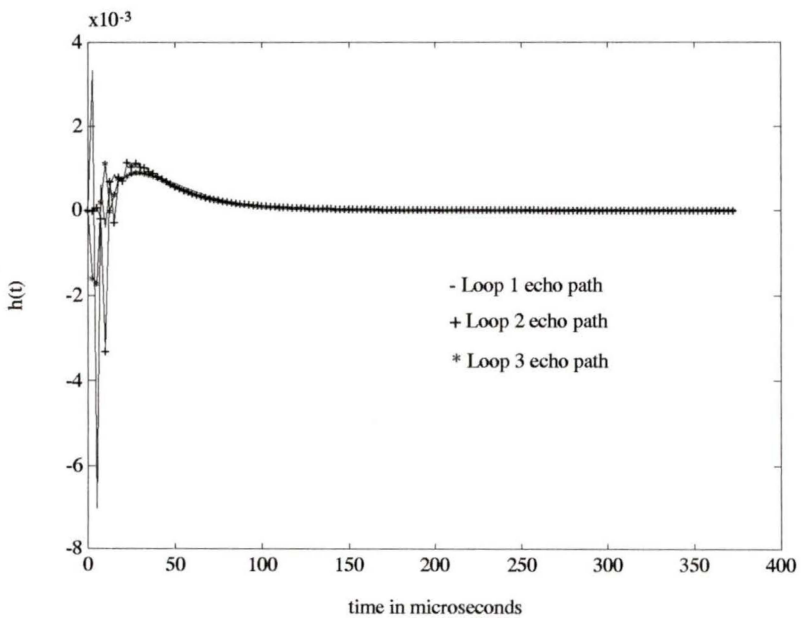

Figure 2.5 Customer-end echo path impulse responses

$$E_{cc} = -10\log\left(\frac{\sum h^2(n) - \sum_{m=0}^{N} w^2(m)}{\sum h^2(n)}\right) \tag{2.5}$$

where

E_{cc} = echo cancellation level in dB

$h(n)$ = echo-path impulse response

$w(m)$ = optimal echo canceler tap weight

N = order of the echo canceler

Using (2.5) the cancellation level for different echo-canceler orders is calculated and the results are shown in Fig. 2.6 and Fig. 2.7 for the central office and customer-end echo paths.

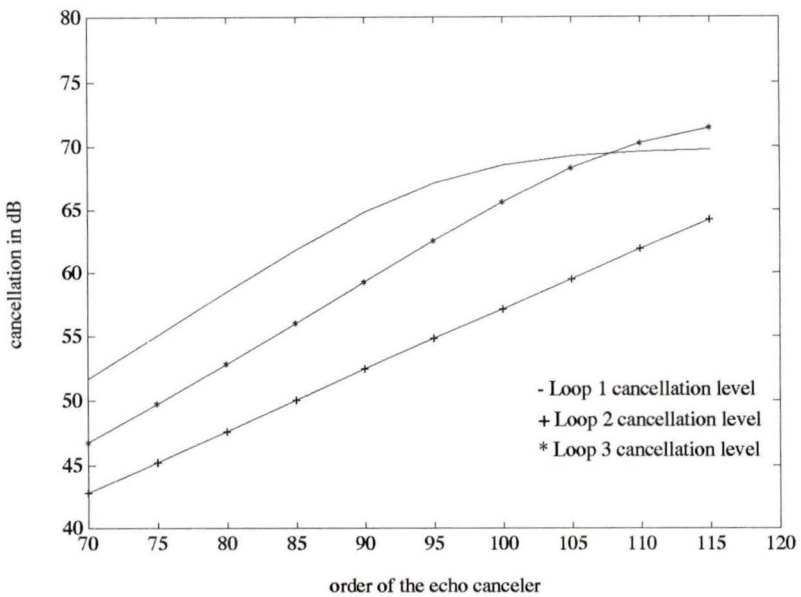

Figure 2.6 Central office echo cancellation

These plots show that a symbol-spaced 100-to-110-tap canceler should provide the necessary cancellation level for most loops under ideal conditions, i.e., assuming the coefficients of the echo canceler can be optimally adapted. As shown in Fig 2.8, the cancellation level does not vary significantly with the sampling phase. The echo

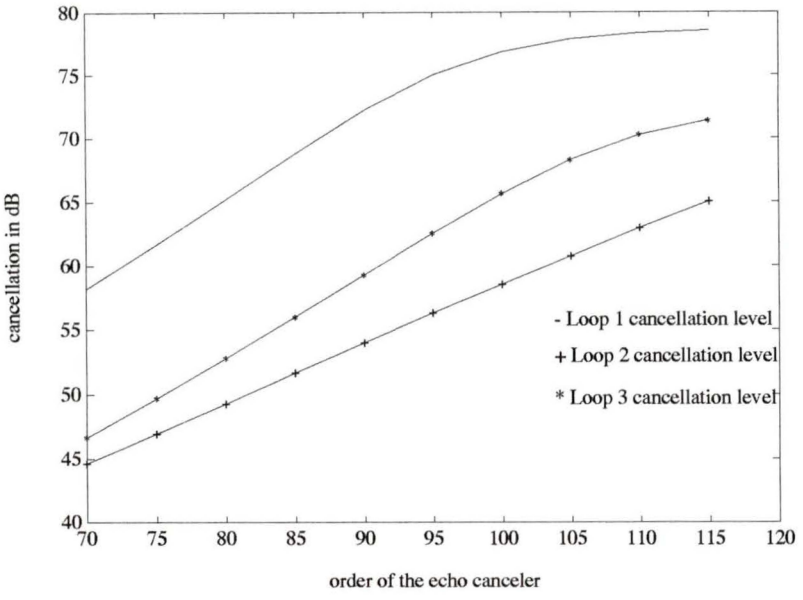

Figure 2.7 Customer-end echo cancellation

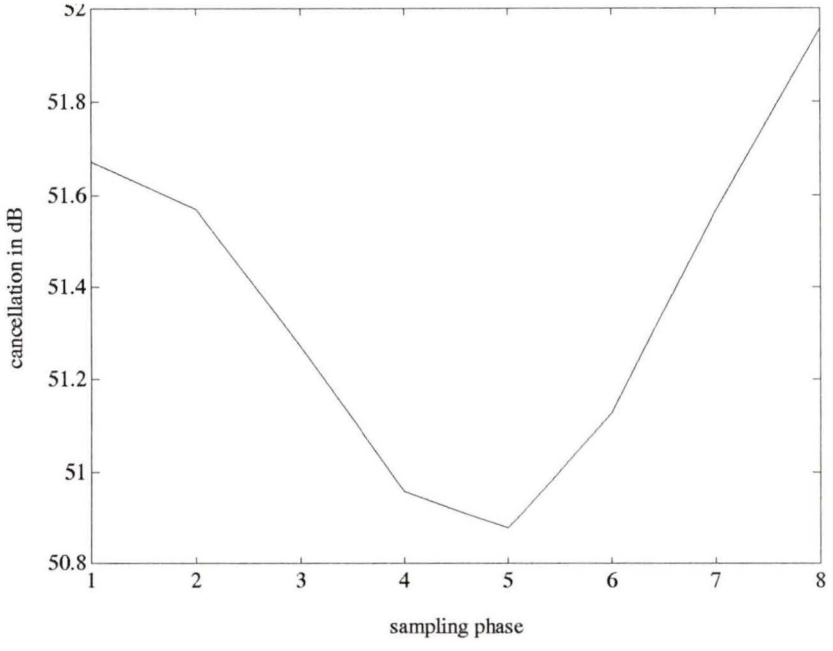

Figure 2.8 Influence of sampling phase on echo cancellation

path was sampled at 8 times the symbol rate and 8 phases were tested using a 90-tap echo canceler for Loop 2 customer-end echo.

These calculations give an estimate of the minimum order of echo canceler needed to achieve the necessary performance level. Since echo paths vary with dif-

ferent lines it is necessary to have an adaptive echo canceler which can be used to achieve the required performance for different lines in the loop plant.

2.3.1 Adaptive echo cancellation

In this section, we describe the simulation details and results of an adaptive HDSL echo canceler. The least mean-squares (LMS) algorithm, being a simple, robust and popular adaptive algorithm [19] will be used in most of our simulations. The reason for using only the LMS algorithm is the fact that other algorithms (RLS, FRLS etc.) are more useful for systems where the input signal is poorly conditioned or in cases where the convergence speed could be seriously affected by the non-stationarities in the environment [19]. In HDSL echo cancellation, the signal input to the adaptive filter is composed of the 2B1Q symbols and since these are generated from scrambled bit sequences [14], the adaptive filter does not suffer from any input ill-conditioning problem. In addition, the echo path does not undergo any significant change over time [12]. Hence there is no special requirement for dealing with non-stationarities.

The echo canceler simulation environment is shown in Fig. 2.9. A 2B1Q generator is used for generating the symbols. The transmit and receive filters are identical 4th-order lowpass Butterworth filters with a 3-dB cutoff at 200 kHz. The echo path is sampled at 8 times the symbol rate and the sampler can be used to select one of the 8 phases of echo. Since the sampling phase does not make a significant difference in the canceler performance we will use one particular phase for the following experiment. The first goal is to obtain an estimate of the order of the LMS echo canceler needed for obtaining the necessary cancellation level for the different echo paths. The convergence characteristics of the echo canceler is also important as it gives an idea

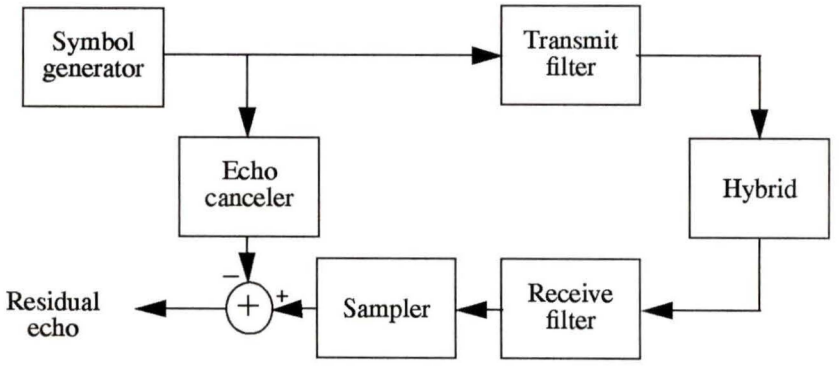

Figure 2.9 Echo-canceler simulation environment

of the time needed to achieve satisfactory echo-cancellation level. The LMS algorithm used is based on the recursive relations

$$e(n) = d(n) - \boldsymbol{w}^t(n-1)\,\boldsymbol{u}(n) \tag{2.6}$$

$$\boldsymbol{w}(n) = \boldsymbol{w}(n-1) + \mu e(n)\,\boldsymbol{u}(n) \tag{2.7}$$

where

$\boldsymbol{w}$ = echo-canceler tap weights

e = error signal used in adaptation

$\boldsymbol{u}$ = symbol input vector into the echo canceler

d = desired response

μ = convergence factor

When estimating the performance of the LMS echo canceler, 10 ensembles of 5000 iterations each were used to obtain the performance characteristics. The maximum value of convergence factor used in these simulations is given by [19]

$$\mu_{max} = \frac{1}{(N+2)\,\sigma_u^2} \tag{2.8}$$

where N is the order of the echo canceler, and σ_u^2 is the variance of the 2B1Q input signal.

In our simulations, the above maximum value of the convergence factor was used in the initial adaptation of the echo canceler and the convergence factor was reduced by a factor of 100 for the last thousand iterations. The degree of cancellation was calculated by obtaining the average of the mean-squared error (MSE) over the last 100 iterations and subtracting this from the value of the return loss provided by the hybrid thereby yielding the amount of cancellation provided by the echo canceler alone. The cancellation level of an echo canceler calculated using the above method is shown in Figs. 2.10 and 2.11 for the central office and customer-end echo paths, respectively, for different orders of the echo-canceler.

As seen from Figs. 2.10 and 2.11, a 110 to 120 tap LMS echo canceler would

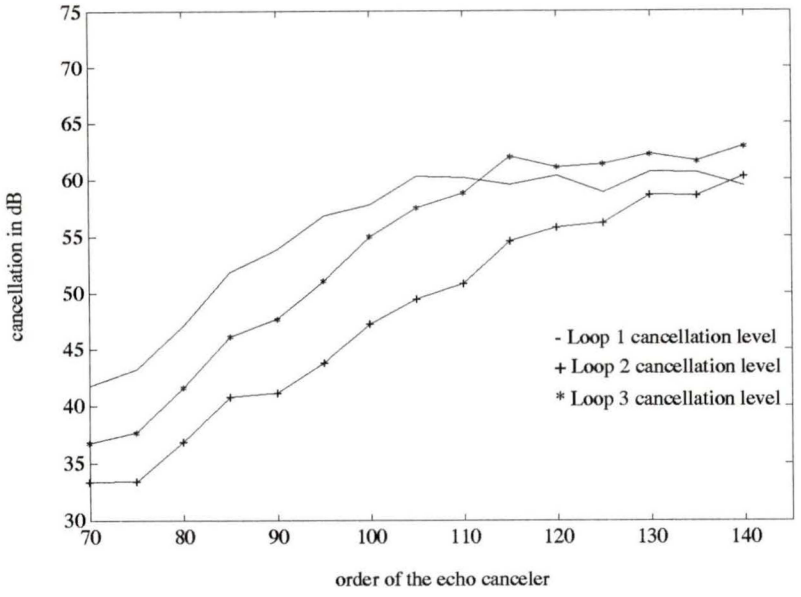

Figure 2.10 LMS echo-canceler performance for central office echo paths

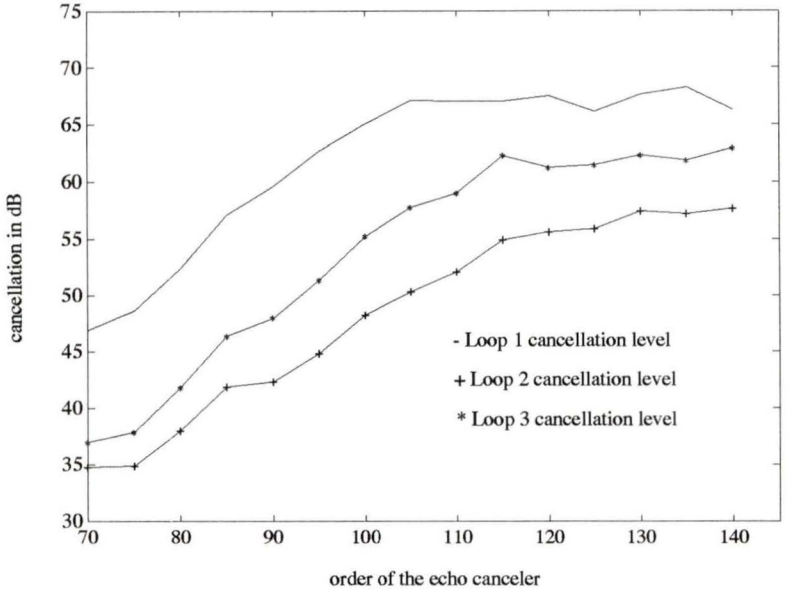

Figure 2.11 LMS echo-canceler performance for customer-end echo paths

be required to enable sufficient degree of echo cancellation for most loops. All these loops are worst-case echo paths (containing the maximum number of bridged taps in CSA loop). The Loop 2 customer-end echo path is the most difficult among the echo paths considered and even though the 60-dB cancellation figure is not met, the cancellation level of 50-55 dB should suffice as this loop does not have a worst case far-end

signal loss. The 60-dB cancellation performance was calculated on the basis of worst-case signal loss which occurs for some loops (e.g., a 12-kft 24-gauge loop or a 9-kft 26-gauge loop). Loop 2 is substantially shorter than these loops and hence the signal loss will not approach the worst-case conditions assumed in [13] for calculating the required echo-cancellation performance.

2.3.2 LMS echo-canceler convergence

The results shown thus far concerning the echo canceler give us an idea of the order of the adaptive echo canceler required to meet the specifications. Only the LMS algorithm has been used in these simulations as it is simple to implement and, as stated earlier, is well suited for this application. In this section we will examine the convergence of the LMS echo canceler.

The convergence of the LMS echo canceler for Loop 2 customer-end echo is shown in Fig. 2.12 for a 120-tap echo canceler. As seen such an echo canceler con-

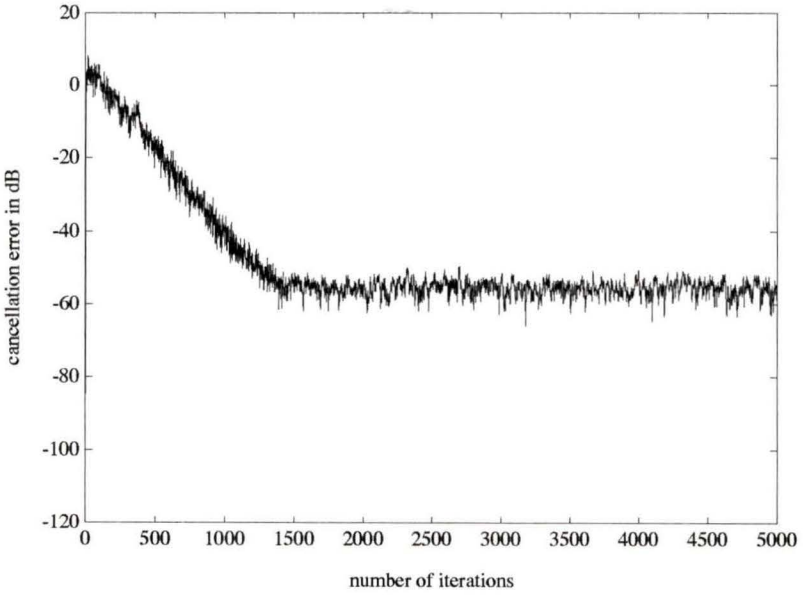

Figure 2.12 LMS echo-canceler convergence

verges after about 2000 iterations. The convergence factor used in this simulation begins with the maximum value of convergence factor given by (2.8) and after 4000 iterations it is reduced by a factor of 100. One point which might be of concern in the simulations presented thus far is the lack of far-end signal in the echo and its effect on the echo cancellation. The simulations were presented with the thought that

the echo canceler would be trained in a noise-free environment (i.e., without far-end signal) before the reception of the far-end sequence. Upon attaining convergence (say after 4 ms) the convergence factor could be reduced to a lower value as in our simulations and the far-end signal could then be received. This simulation also assumes that the timing jitter in the clock at the receiver is very small; otherwise, the following scenario could result.

In the training scheme presented above, the echo canceler was trained with a particular timing phase. However, after the convergence factor is reduced following satisfactory convergence any phase change will result in a very poor cancellation level. This is shown below in Fig. 2.13 for Loop 2 customer-end echo where the change of phase results in very poor cancellation. In this experiment, the LMS echo-canceler was simulated for phase 1 using the method outlined above and then the converged tap-values were retained with the reduced convergence factor and the echo cancellation for the other 7 phases were simulated.

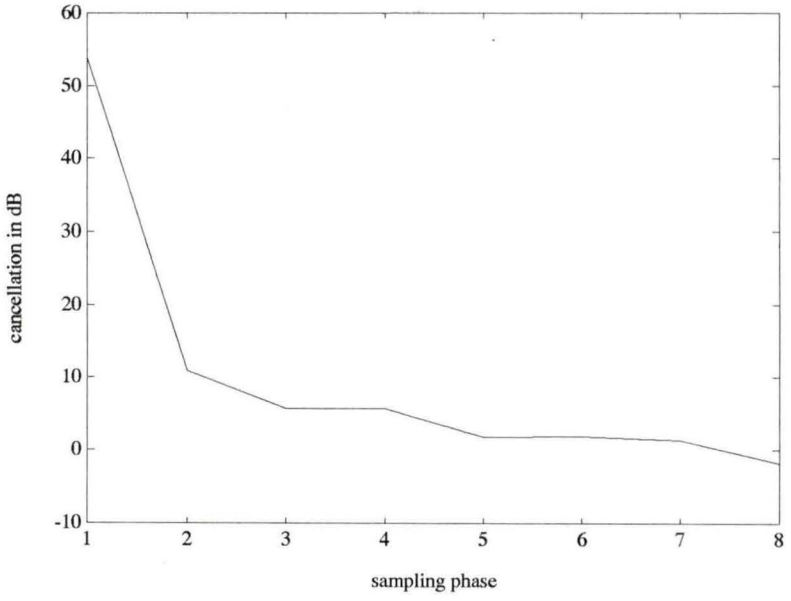

Figure 2.13 Effect of timing jitter on proposed echo cancellation method

2.4 Analysis of the Echo Path

A typical HDSL echo-path response has certain features which can be exploited to reduce the order of the echo canceler in the transceiver. A detailed look at the different echo paths shows some interesting similarities. Typically, as shown in Figs. 2.4

and 2.5, any echo path has an initially random portion followed by a predictable tail portion. The initially varying portion in the echo path is dominated by reflections from the bridged taps. In Fig. 2.14, the severity of randomness in the initial part of the echo path can be seen to vary depending on the number of bridged taps. The

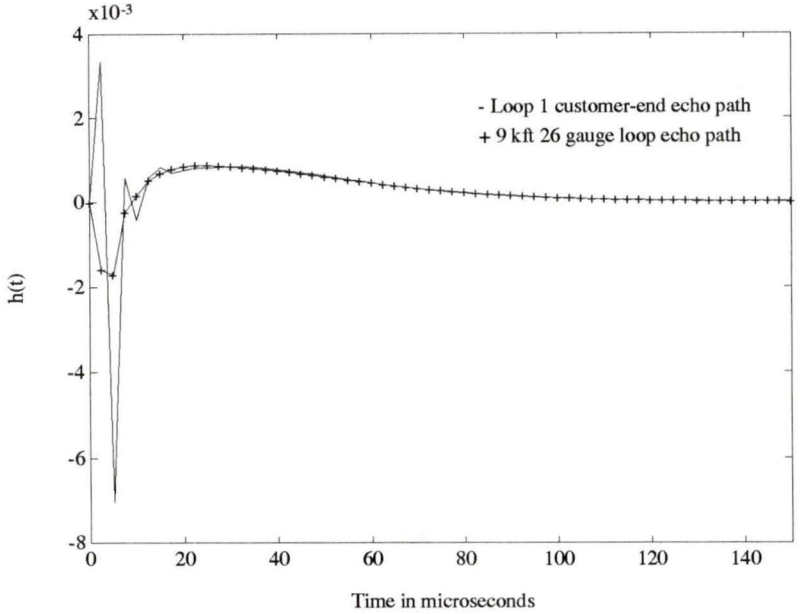

Figure 2.14 Comparison of echo paths with respect to bridged taps

major portion of the echo path is the slowly varying tail evident in the different echo paths. This slowly decaying tail is caused mainly by the line transformer in the signal path. The transformer model in Fig. 2.3 shows a 3 mH primary inductance. The order of the echo canceler needed to obtain satisfactory performance is affected by this value of the primary inductance since the echo path response decays more slowly for transformers having a higher value of primary inductance. This is illustrated in Fig. 2.15 where the echo tails are shown for different inductances. The lower value of inductance is preferred to a higher value since it reduces the echo-canceler order and, therefore, a lower amount of computation is required to achieve the performance criterion. Moreover, the primary inductance value of 3 mH used in our work has been also shown to satisfy the linearity requirements [13].

The standard echo-canceler order needed in the HDSL system was found to be around 110-120 taps for satisfactory performance. Since economic viability is a major factor in the design of the HDSL system, other techniques which may help in reducing the order are investigated.

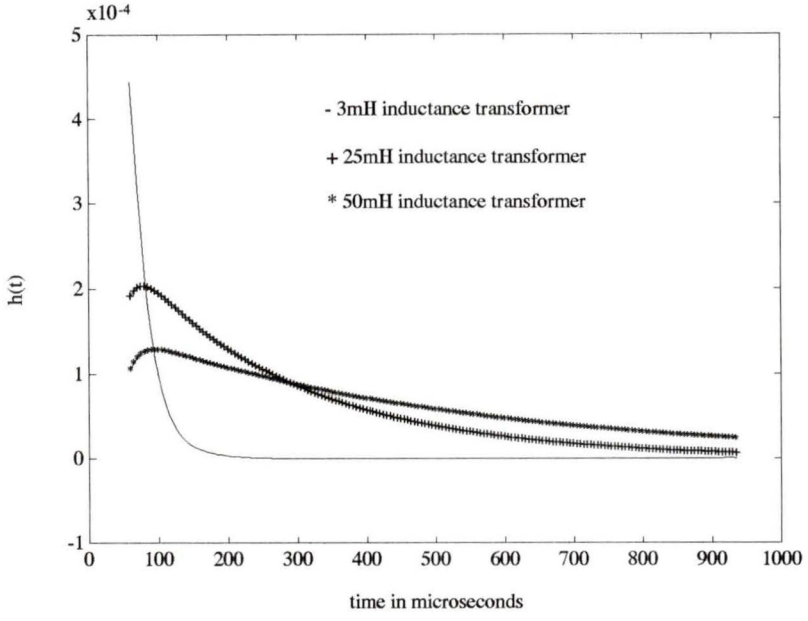

Figure 2.15 Echo-tail comparison for different transformer primary inductances

2.5 Reduced Order Echo Cancellation

The analysis of the echo paths revealed two important features present in most of the echo paths. The initial part, caused by reflections in the loop plant are unpredictable due to the presence of gauge changes and bridged taps. The second part though is heavily influenced by the transformer and has the same characteristic in all the echo paths in the loop plant. This is shown by the fact that there was a very similar decay in all the echo paths investigated. This long decay is largely responsible for such long canceler orders seen in the previous sections. Hence our approach is to study the transformer characteristics for canceling the tail portion of the echo with significant reduction in the order of the echo canceler.

2.5.1 Echo cancellation using highpass filtering

The echo-path transfer function is given by (2.1). The slowly decaying tail portion in the echo paths can be assumed to be caused by a dominant pole in the echo-path transfer function as has been done in [20] for channel-tail cancellation for equalization purposes. We analyze the echo-path transfer function and approximate the dominant pole causing the decaying tail in Appendix 1. The approximate dominant pole position is found to be around 3 kHz and to reduce the effect of this pole in the echo, and, consequently, the echo-canceler order, attenuation near this pole frequency can

be used. We propose a highpass filtering technique for achieving this goal. The effectiveness of this method is tested by obtaining simulation results on the echo paths used in the previous sections. The only change from the simulation model shown in Fig. 2.9 is the introduction of the highpass filter in the receive path. In our experiments, we use a 4th-order Butterworth highpass filter with different cutoff frequencies.

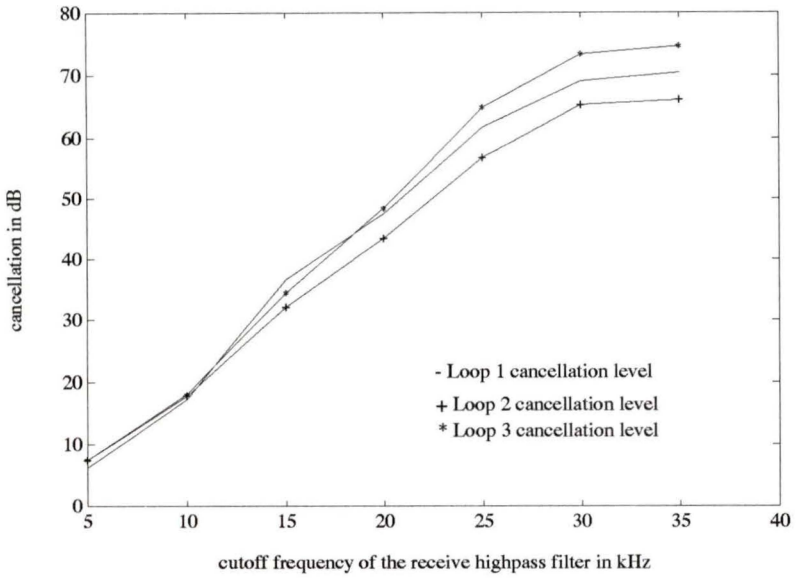

Figure 2.16 Echo cancellation with a variable cutoff highpass filter for central office

There are two parameters which can be studied with the highpass filter in the receive path. Since the objective of the method is to reduce the order of the echo canceler needed in a HDSL system, the order will be estimated using simulations. Additionally, the cutoff frequency of the highpass filter in the receive path is studied in the simulation. In the first simulation, the cutoff frequency of the high-pass filter is varied for a fixed-order echo canceler (60 taps) for the different echo paths. The results are presented for the central office and customer-end echo paths in Figs. 2.16 and 2.17.

These plots show that using a highpass filter with a cutoff frequency around 20-25 kHz and an echo canceler of 50-60 taps should provide sufficient cancellation performance. Moreover, the complexity (in terms of extra hardware) increase due to this highpass filter in the echo path is minimal as the lowpass receive filter could be combined with a suitable highpass filter characteristics to achieve a single receive fil-

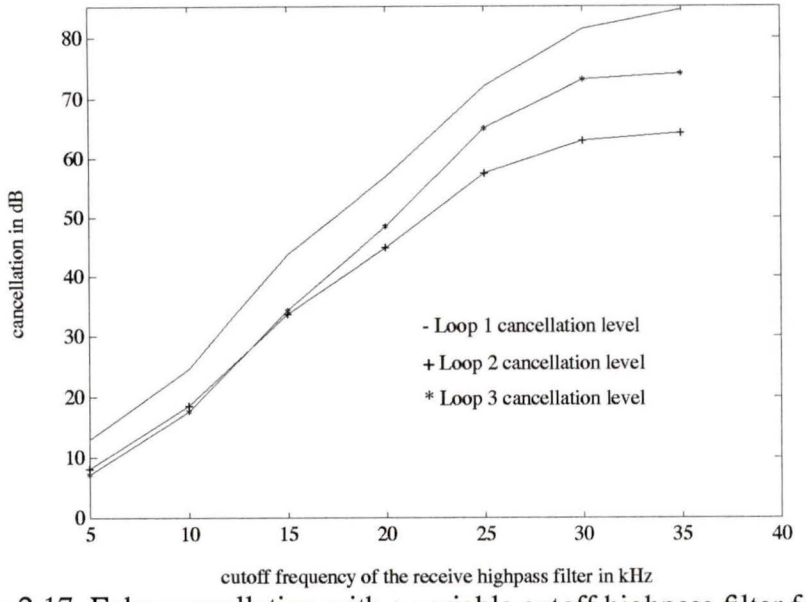

Figure 2.17 Echo cancellation with a variable cutoff highpass filter for customer end

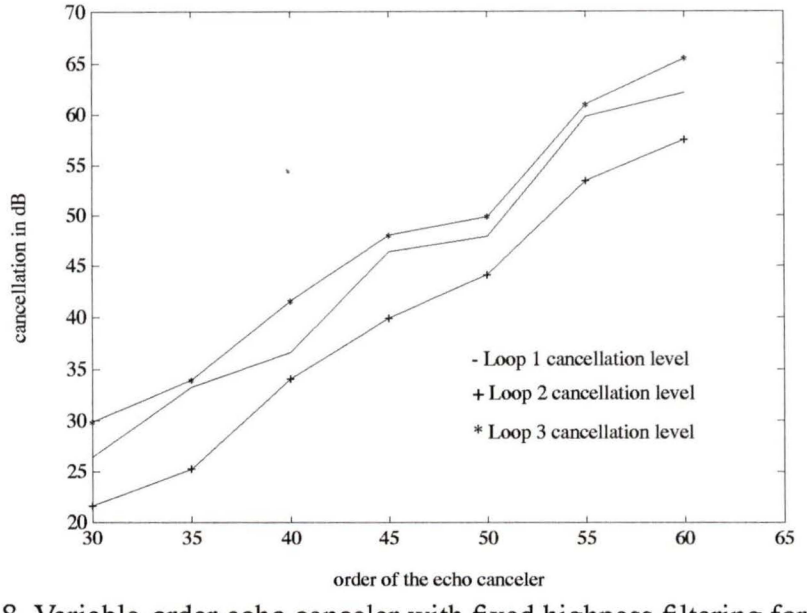

Figure 2.18 Variable-order echo canceler with fixed highpass filtering for central office echo cancellation

ter. In the second experiment with the highpass filter, the echo-canceler order is varied for a fixed receive highpass filter (25 kHz cutoff). The results are shown in Figs. 2.18 and 2.19.

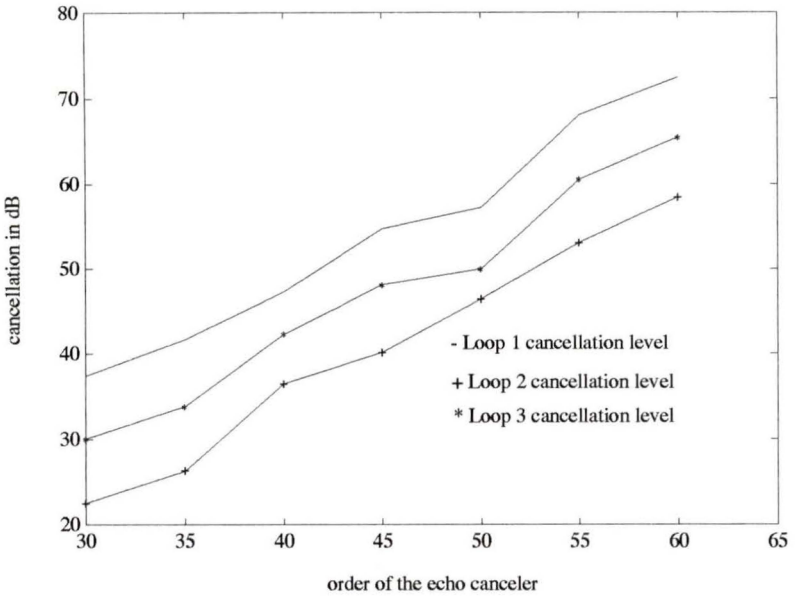

Figure 2.19 Variable-order echo canceler with fixed highpass filtering for customer-end echo cancellation

2.5.2 Echo cancellation using pole cancellation

For the second technique we use the s-domain pole position obtained in the analysis of the echo-path transfer function. This pole is converted into a z-domain pole using the bilinear transformation [21] and a zero is placed at this pole position, realized as a two-tap filter in the echo-receive path. This method is targeted towards canceling the effects of the dominant pole which causes the long tail in the echo paths. Some simulation results that verify the effectiveness of the technique are illustrated in Figs. 2.20 and 2.21. These plots show the cancellation level achieved by the echo canceler as a function of the order of the echo canceler. The benefits of this method are evident from the fact that a 50 to 60-tap echo canceler can be used to achieve the required level of cancellation.

The preceding two techniques have helped in reducing the order of the echo-canceler by a significant amount in all of the echo paths investigated. The results for the two new techniques are presented in Table 2.1 along with the results for the standard echo canceler. The pole cancellation method has been observed to be crucially dependent on the pole position obtained using the analysis in Appendix A. Hence an accurate model of the hybrid and the transformer might be needed for achieving the performance presented.

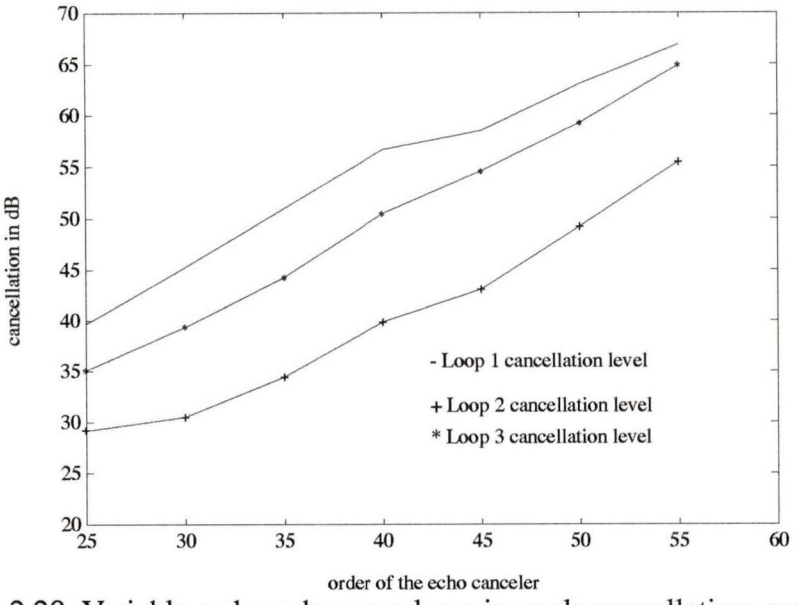

Figure 2.20 Variable-order echo canceler using pole cancellation: central office echo cancellation

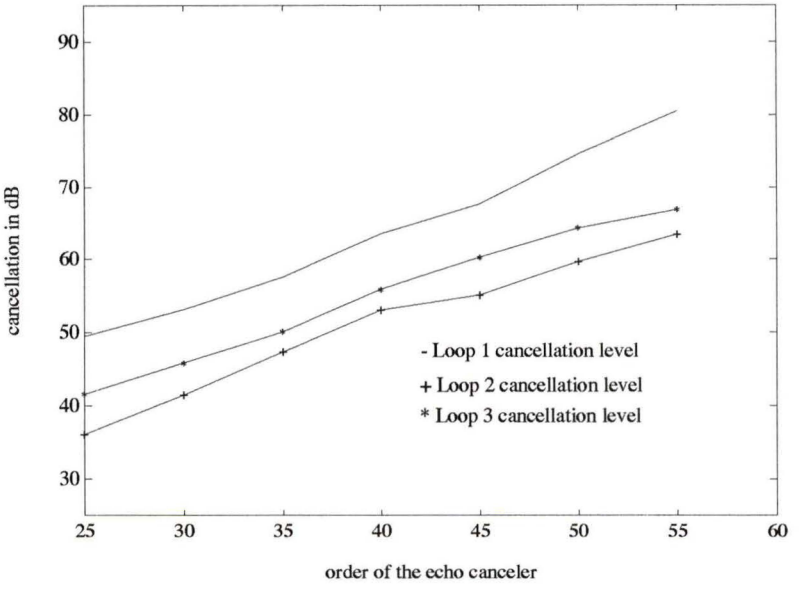

Figure 2.21 Variable-order echo canceler using pole cancellation: customer-end echo cancellation

2.5.3 Higher-rate echo cancellation

In an HDSL transceiver, the echo canceler has to co-exist with the equalizer. The relative positioning of these two elements is an important issue in the design of the transceiver [22] but is not the focus of this thesis. For a variety of reasons the echo

cancellation could be performed before the equalization [22]. This necessitates consideration of some issues in the design of the echo canceler.

Table 2.1 Comparison of different echo cancellation techniques

Loop	EC	SEC	HP	HP savings	PC	PC savings
Loop 1 (CO)	60 dB	120	57	52.5%	48	60%
Loop 2 (CO)	55 dB	125	60	52%	55	58%
Loop 3 (CO)	60 dB	112	55	50%	52	53.5%
Loop 1 (CE)	60 dB	90	50	44%	37	58.8%
Loop 2 (CE)	55 dB	130	57	56%	48	63%
Loop 3 (CE)	60 dB	115	55	52%	55	52%

CO = Central office

CE = Customer end

EC = Echo cancellation level

SEC = Standard echo canceler order

HP = Order of the echo canceler with high pass filtering

PC = Performance of pole cancellation method

A symbol-spaced equalizer (SSE) can be used along with an symbol-spaced echo canceler but a fractionally-spaced equalizer (FSE) needs an echo estimate at the specified fraction of the symbol period. One simple solution to this problem is to have a fractionally-spaced echo canceler spanning the desired number of symbols. From our previous experiments we can predict that a 240 to 250-tap T/2 echo canceler is needed to provide a satisfactory echo estimate to co-exist with a T/2 equalizer. Implementation of a 250-tap canceler at such a small tap spacing might be technologically demanding and expensive. Another issue is that the input into a T/2 echo canceler is not the 2B1Q symbols as a higher rate input is needed at the echo canceler. This could result in much more complex hardware in echo-canceler implementation [10]. Hence other techniques which obviate such complexities are investigated.

2.5.3.1 Interleaved echo canceler

Interleaved echo cancellation was proposed in [10] for solving the above problem of producing a higher than symbol-rate echo estimate without implementing a T/*m* spaced echo canceler. In this method, *m* symbol-spaced echo cancelers are used for achieving an *m* times symbol rate echo estimate. The individual SSEs are used to cancel the different epochs of the echo. This is illustrated in Fig. 2.22 for an echo canceler which is needed to interface with a T/2 FSE. A simulation model based on [10] was implemented for testing this method in a HDSL system. The simulations

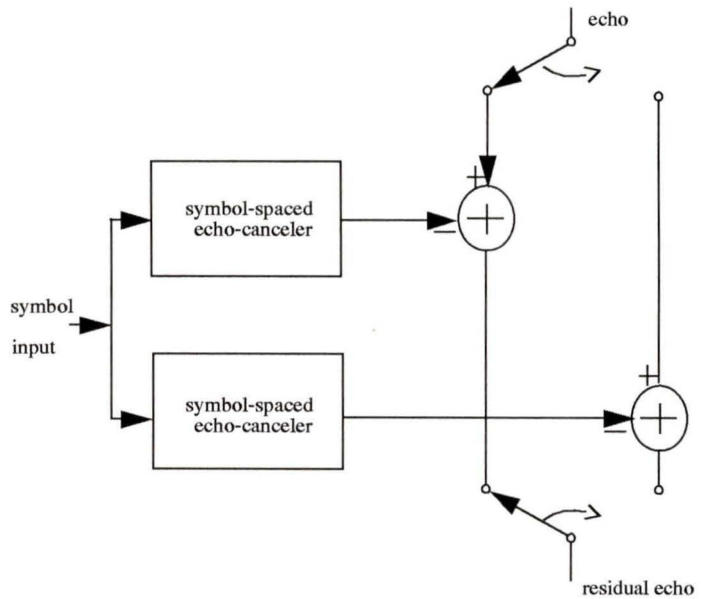

Figure 2.22 Interleaved echo cancellation

were performed for the Loop 2 customer end echo path. The order of the symbol-spaced echo cancelers and their respective cancellation performance are illustrated in Fig. 2.23. As shown in Fig. 2.22, two symbol-spaced echo cancelers are required for interfacing with a T/2 FSE. Highpass filtering in the echo path helps reduce the order of the echo canceler and results in savings in the region of 100 taps (around 50 taps for each canceler) for the echo paths investigated and this is demonstrated in Fig. 2.24 where a a highpass filter with a 25 kHz cutoff is used.

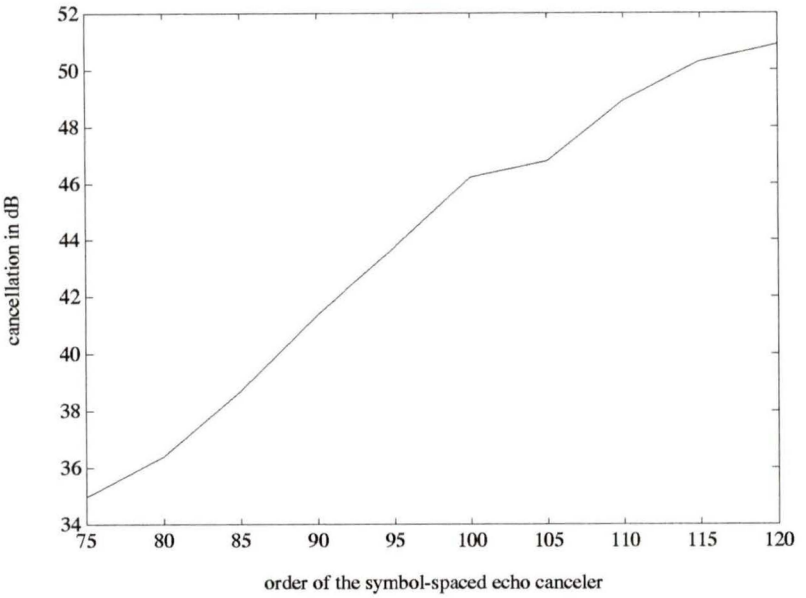

Figure 2.23 Performance of an interleaved echo canceler for Loop 2 customer-end echo

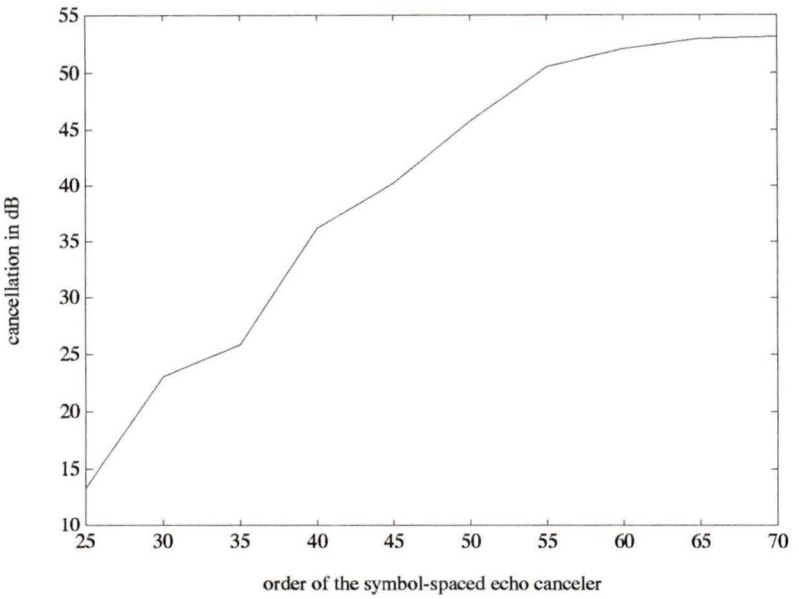

Figure 2.24 Performance of an interleaved echo canceler with a highpass filter for Loop 2 customer-end echo

2.5.4 Echo tail cancellation using orthonormal functions

In [23], a technique is proposed for canceling long echo tails in DSL. In this method, the echo tail is represented as a combination of orthonormal functions. The echo canceler is split in two parts in which the first part is used to cancel the initial part of the

echo and the second part is a tail canceler based on orthonormal functions, which is used to cancel the long echo tails.

This method is a two-stage echo cancellation technique. In the first stage of the echo cancellation a standard FIR echo canceler is used to match the random portion path in the echo path impulse response. The order of the filter used in the first stage of the echo cancellation is N_a.

In [23], the echo paths investigated had very long tails which spanned almost 1000 symbol intervals. Hence the echo tail was approximated by a linear combination of orthonormal functions. These functions were chosen such that they could be implemented by simple recursive filters. These sets of recursive filters form the second part of the echo cancellation. The number of orthonormal functions used is given by N_b. The signal input into the second part of the echo canceler is real, unlike the symbol input to the first part. As a result real, multiplications need to be used in the implementation of this echo canceler.

The number of real multipliers needed in this method is proportional to N_b. A

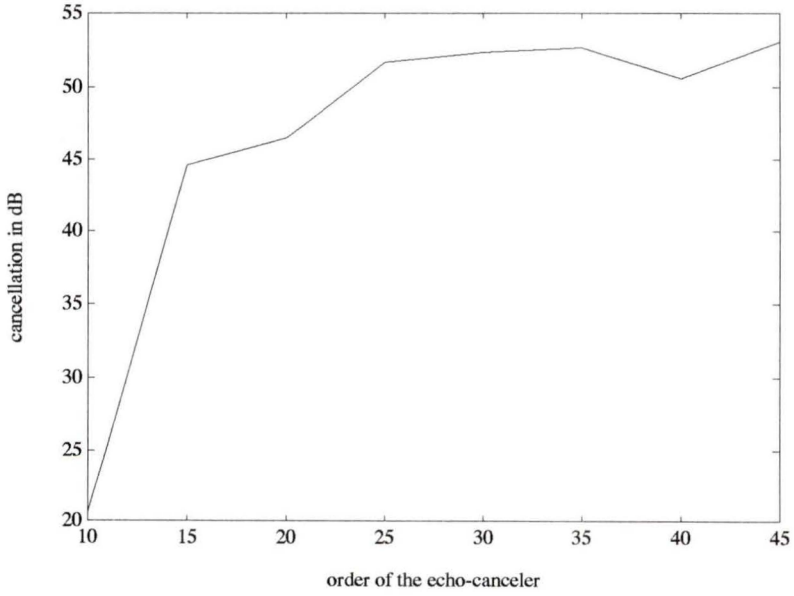

Figure 2.25 Orthonormal functions based echo-canceler performance

simulation model for this technique was designed based on the method outlined in [23] and the performance for a orthonormal tail canceler with varying canceler order is presented in Fig. 2.25 for a fixed N_b = 5 and varying echo-canceler order. The

Loop 2 customer-end echo path was used in the simulation.

It was found that a 30 to 35-tap echo canceler has to be used in conjunction with an orthonormal tail canceler to achieve the cancellation performance of 50 to 55 dB. The orthonormal tail canceler needs multipliers of the order of $5N_b$ and hence 25 multiplications are needed in this particular case. In our simulations we tried to reduce the order of the tail canceler but this was the minimum possible order necessary for achieving satisfactory performance characteristics. These results show that the orthonormal tail canceler will result in echo cancelers which need real multipliers, unlike the cancelers using highpass filtering methods which were proposed in this work.

2.5.5 Interpolated FIR tail canceler

A new technique using an AIFIR for DSL echo cancellation was proposed in [17][24]. The premise of the technique is that long echo tails which have narrowband frequency responses can be synthesized using sparse filters as proposed in [25]. A block diagram representation of this idea is shown in Fig. 2.26. The transformer

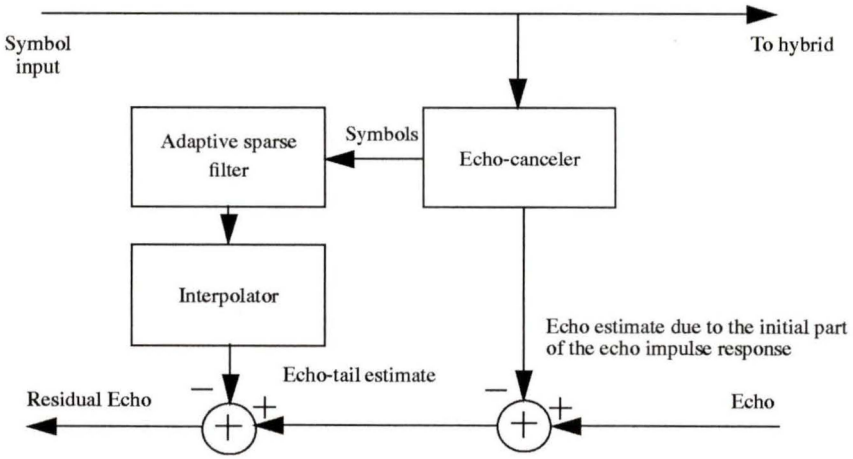

Figure 2.26 AIFIR technique for echo cancellation

model used in [17] has a 50 mH primary inductance and, as a consequence, very long echo tails are present. The AIFIR filter has three separate sections which are used in the echo cancellation. A symbol-spaced echo canceler is used to model the initial random portion of the echo path. The long decaying tail part is modelled by a sparse filter and the output is interpolated using a fixed interpolator to obtain an estimate of the echo-path tail. As seen from Fig. 2.26, the interpolator does not have symbols as

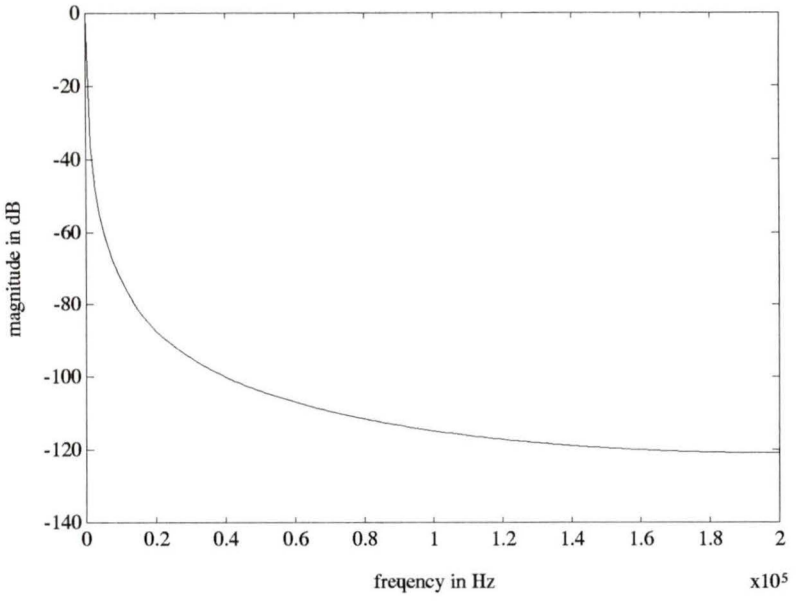

Figure 2.27 Echo-path tail frequency response for a large primary inductance transformer

input and needs multipliers for implementation. Before embarking on the simulation of the AIFIR technique for our echo models, the tail frequency responses were analyzed and are shown in Figs. 2.27 and 2.28. The responses in the plots show the narrow bandedness of the echo tail corresponds to a high value primary inductance. The

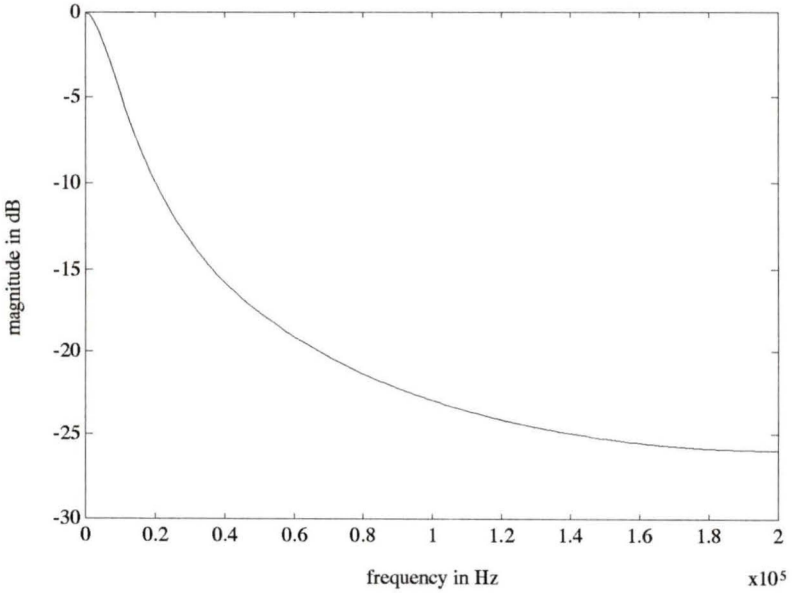

Figure 2.28 Echo-path tail frequency response for a small inductance transformer

AIFIR technique is not suitable for the echo paths used in this work because the echo tails are short as compared to the echo tails in [24] and as a result they are not as narrow in the frequency domain. Therefore, the extra hardware in the form of real multipliers which is needed in the case of a AIFIR tail canceler cannot be justified.

2.6 Conclusions

In this chapter, HDSL echo cancellation was examined in detail. Our research shows that classical LMS echo cancelers of 110 to 120 taps can be used to provide sufficient performance under the required conditions. Moreover, the order of the echo canceler can be greatly reduced by the use of highpass filtering or by using knowledge of the transformer characteristics. This was demonstrated and a comparison with two proposed techniques illustrates advantages of the proposed method. The interfacing of a symbol-spaced echo canceler with a FSE was also considered. Interleaved echo-cancelers were explained and successful performance was achieved for HDSL echo cancellation. This enables interfacing an echo canceler with a T/2 spaced equalizer.

Chapter 3

HDSL Equalization

3.1 Introduction

One of the main challenges in the HDSL system implementation is the NEXT from other signals in the same multi-pair cable and the ISI caused by the high transmission rates in the subscriber loop channel [26]. The copper wire-pairs in the subscriber loop plant were originally designed for analog voice communication. For transmission of high-frequency signals as in the HDSL system, several impairments in the channel have to be overcome.

In T1 transmission, cables with repeaters placed along the route are used to enable high-speed transmission [2]. The reasons for using the HDSL system in place of T1 are largely economic and have been outlined in previous sections. The subscriber-loop plant has very high attenuation at the HDSL system frequencies [6]. Moreover, the short symbol spacing results in significant ISI at the receiver [22]. Traditionally, equalizers have been used to overcome the above impairments [9]. In high-rate transformer coupled lines, as in HDSL, there is a significant post-cursor tail in the channel impulse response which could cause significant ISI [22]. DFEs are used to overcome this problem effectively and efficiently as linear equalizers cannot equalize such channels successfully [8].

FSEs have been found to have better performance with respect to sampling phase [27] and, as will be explained in a later section, can have better crosstalk suppression characteristics under certain conditions. In this chapter, the focus is on studying the HDSL equalizer in the presence of ISI and NEXT. A general overview of advances in the area of equalization is presented in the second part of this chapter. The modeling of the channel and the crosstalk for the HDSL system is then explained and simulated. Some useful ideas on the nature of crosstalk in different synchronization conditions are pre-

sented.

A recently developed theory for cyclostationary crosstalk suppression is explained with relevance to HDSL. This is used to achieve a successful equalization strategy satisfying prescribed performance standards. The use of highpass filtering in reducing the complexity of the echo canceler was explained in chapter 2 and the inclusion of the highpass filter in the signal path (for testing the performance of the equalizer) is also simulated. Decision-directed equalization is also studied and an estimate of the training lengths needed in practical HDSL equalizers is obtained using simulations.

3.2 Equalization

Some general information on equalization is presented before proceeding with the specific task of HDSL equalization. The subscriber loop has frequency-dependent attenuation which increases rapidly with frequency as shown in Fig. 3.1 for a 13-kft

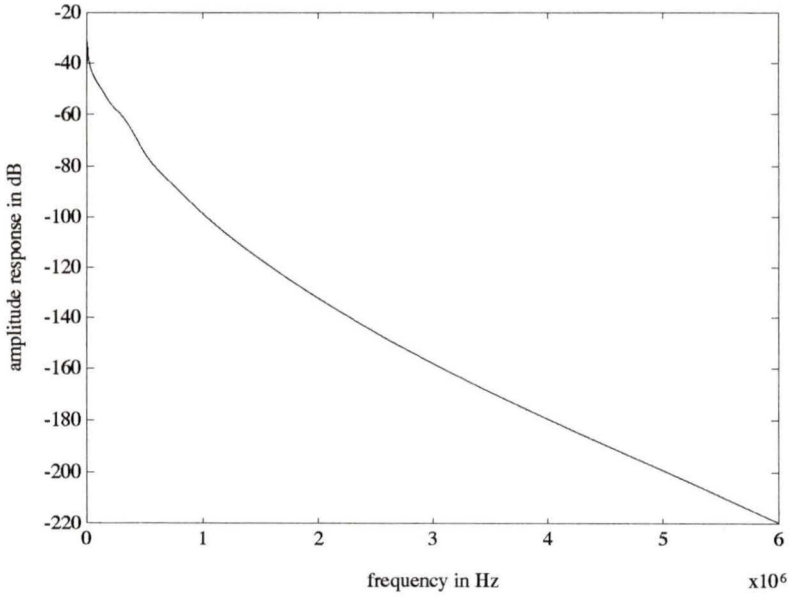

Figure 3.1 Magnitude response of a 13-kft 24-gauge loop

24-gauge loop. The phase characteristics (though linear in most of the band) also contribute to the temporal dispersion of the signals transmitted over this frequency range. In bandwidth-efficient digital communications systems, the effect of each

symbol transmitted over a time-dispersive channel extends beyond the time interval used to represent the symbol. The distortion caused by the resulting overlap of received symbols is called ISI. This is a major impediment in systems like HDSL which transmit high data rates over channels of limited bandwidth such as the subscriber loop. The severe ISI in HDSL is because of the short symbol spacing which causes many symbols to contribute to the ISI.

Equalization, which dates back to the use of loading coils to improve the characteristics of twisted-pair telephone cables for voice transmission, is used to compensate for these non-ideal characteristics by filtering. In transformer-coupled channels such as HDSL, the channel impulse response (shown in Fig. 3.6) may have a long tail (post-cursor) which would contribute toward a significant amount of ISI. The ISI in such channels can be divided into two parts called the pre-cursor and post-cursor ISI. Precursor ISI is the interference caused by the portion of the channel impulse response before the cursor and the postcursor ISI is caused by the portion of the channel impulse response after the cursor.

In a simple linear equalizer, the ISI is overcome by a filter which has frequency characteristics to compensate for the distortions in the channel as shown in Fig. 3.2.

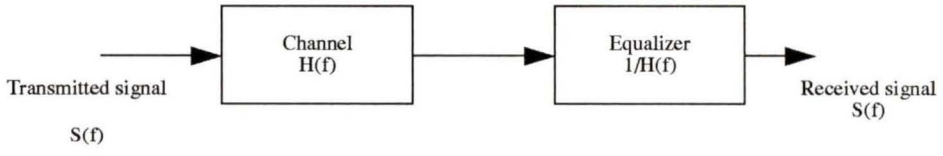

Figure 3.2 Simple illustration of linear equalizer operation under ideal conditions

Adaptive equalizers can be used for tackling various channels (e.g., different lines in the subscriber loop plant) and can also track variations in the individual channels themselves [9].

Minimum mean-squared equalizer (MMSE) linear equalizers are designed to cancel ISI in the presence of noise. In subscriber loop channels with transformer coupling, there is a significant post-cursor tail and the ISI caused by such a tail increases with transmission rate. A simple technique was proposed in [8] for cancelling the interference caused by this tail as shown in Fig. 3.3. Since the symbols causing the post-cursor ISI are detected prior to the present symbol, their effect on the present

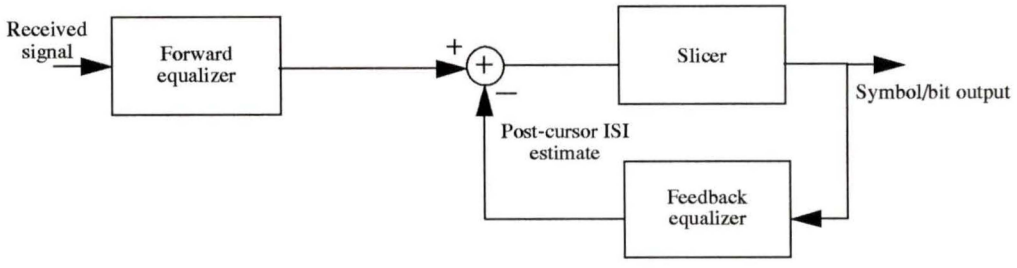

Figure 3.3 Illustration of DFE operation

symbol can be cancelled by a feedback equalizer. Such a feedback equalizer models the post-cursor of the channel after forward filtering. The feedback equalizer's advantage is based on the fact that the detected symbols up to the present instant are correct with a high degree of reliability. Such reliable transmission requirements can be established only after a suitable training period. Bit-error bursts can occur under certain conditions as an incorrect symbol fed back could cause a chain of errors but detailed studies have been performed on this [8] showing that it is not a significant problem. Practical DFE systems have been used in many applications and have resulted in better performance when compared to a linear equalizer [28]. Since the feedback equalizer's input is the symbol sequence, simplified filter realization is possible as compared to a linear equalizer as the latter needs real multipliers for implementation. Thus a DFE is used to reduce the requirements of the forward filter thus reducing the sensitivity of the equalizer to noise and sampling phase [9]. All of this can be achieved at no substantial increase in complexity. In the HDSL system, DFEs will be used for all the above-mentioned reasons.

A linear equalizer acting alone or with a feedback equalizer is normally tap-spaced at the symbol/bit period of the system. However, non-ideal receive filtering results in received signals having energy above the Nyquist frequency. As a consequence, the symbol-spaced forward filter could suffer from aliasing at the forward filter's input which is manifested in performance degradation at certain sampling phases [29]. The tap spacing in the forward equalizer can be made lesser than the symbol spacing as shown in Fig. 3.4 to overcome this aliasing problem and consequently provide consistent performance with respect to the sampling phase. The adaptation rate of the FSE remains the same as for a SSE. Another advantage of such an equalizer is the crosstalk suppression (under certain crosstalk conditions) possible

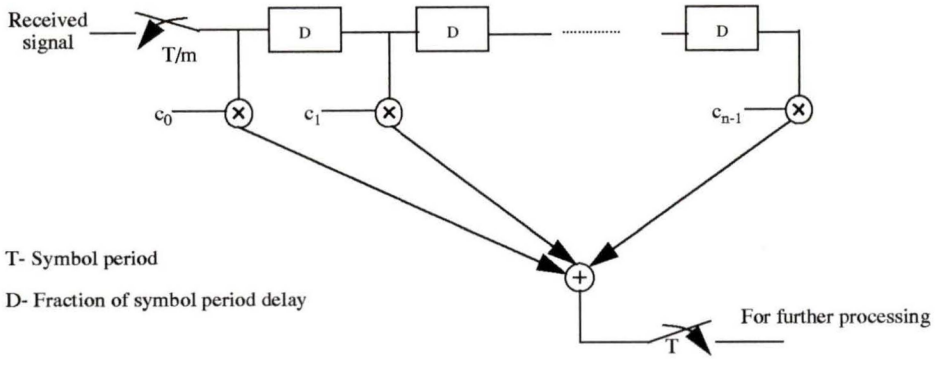

Figure 3.4 Illustration of the operation of a FSE

due to the extra bandwidth available and this will be detailed later. These are some of the general ideas in the field of equalization and some of these will be used in HDSL equalization.

3.3 Channel Modeling

A channel model is necessary for studying the HDSL equalizer performance. We consider one worst-case loop, a 13-kft 24-gauge loop, for testing the performance of the equalizer. This is longer than the longest loop in the CSA population (12-kft 24-gauge) and a satisfactory equalizer performance for this loop should ensure satisfactory performance in the CSA population. The longer loop will also give some extra performance margin for the simulation results presented.

The modeling of the line can be illustrated as in Fig. 3.5 where the *ABCD* parameters of the line and the transformer are obtained as described in the previous

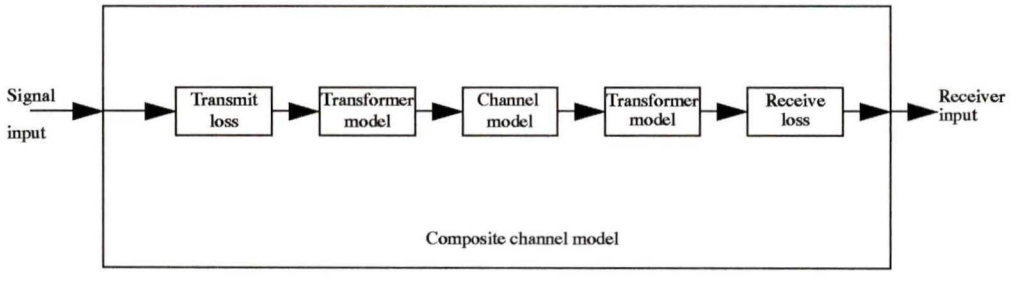

Figure 3.5 Channel modeling procedure

chapter. The frequency response of the channel along with the transformers is obtained as

$$H = \frac{Z_l}{Z_o(Z_l C_l + D_l) + A_l Z_l + B_l} \tag{3.1}$$

where the quantities involved in the equation have been defined in chapter 2.

The transmit and receive loss are due to the hybrid used in the transceivers. They are given as

$$H_{tl} = \frac{Z_o}{Z_o + Z_{in}} \tag{3.2}$$

and

$$H_{rl} = \frac{Z_{in}}{Z_o + Z_{in}} \tag{3.3}$$

respectively. The hybrid equivalent circuit outlined in chapter 2 was used in the above equations. The channel frequency response obtained in (3.1) is multiplied by the loss functions to obtain a complete frequency-domain description of the channel. The IFFT is then used to obtain the impulse response of the channel and this is illustrated for the 13-kft 24-gauge loop in Fig. 3.6. An interesting observation made with regard to the impulse response of the channel is the post-cursor tail. Comparisons with channel responses obtained for similar lines in [40] and in [43] revealed that the post-cursor in our channel model is considerably shorter than most responses used by other research groups investigating HDSL equalization. This is due to the influence of the large primary inductance in the transformer which has been used in the channel modeling. Hence a shorter feedback equalizer length could be expected in our simulations.

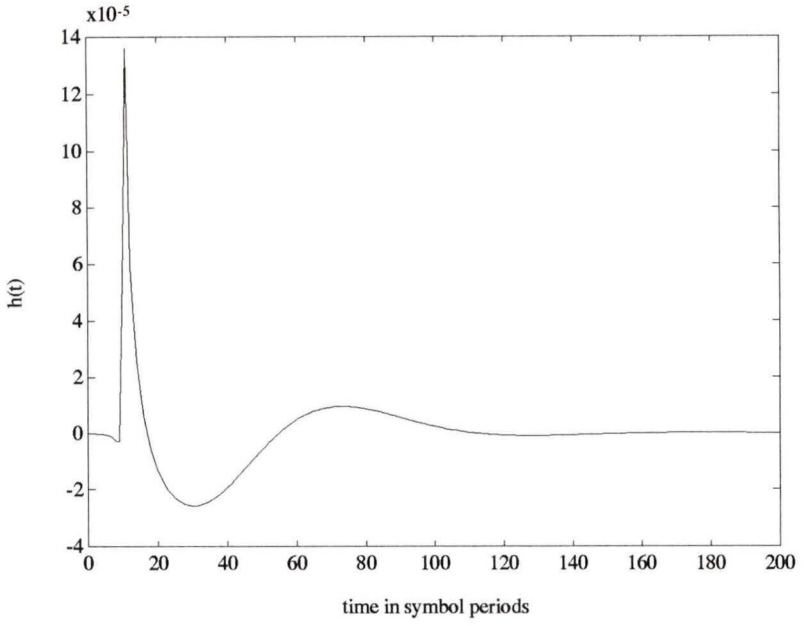

Figure 3.6 Impulse response of a 13-kft 24-gauge loop

3.4 Crosstalk Modeling

The NEXT forms the limiting factor in the determination of maximum allowable loop lengths in HDSL [6]. The different forms of crosstalk existing in the loop plant are shown in Fig. 3.7. The multi-pair cables in the subscriber loop plant can contain a maximum of 50 lines each of which can be used for different services as indicated in the above figure. Some of the typical services are analog voice, basic rate ISDN,

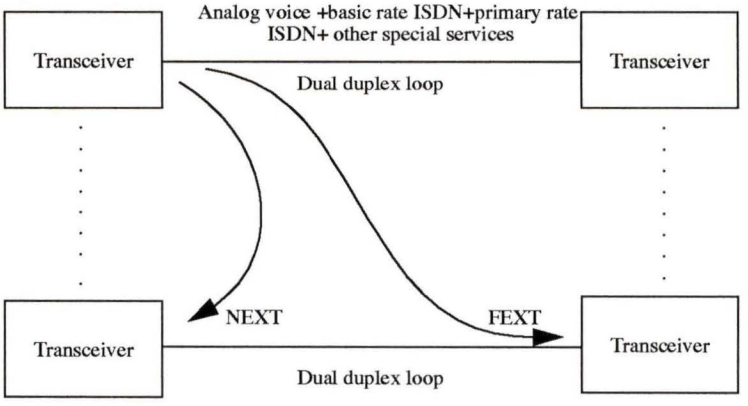

Figure 3.7 Crosstalk environment in the subscriber loop plant

and HDSL. Interference from all these signals can occur in a HDSL environment. Moreover, the crosstalk can be NEXT or and far-end crosstalk (FEXT) which are illustrated in Fig. 3.7.

NEXT is interference from the same end transceivers and is predictably more damaging than FEXT because of the line loss suffered by the far-end signal. The most damaging interference occurs due to self-NEXT which is caused by other similar HDSL transmitters using the same cable [6]. Typically, there are 50 lines in a single cable, and as was stated earlier, in a worst-case scenario, all other lines could have HDSL transceivers causing crosstalk into one receiver. We will consider this worst-case scenario of 49 interferers in our equalizer simulations. The worst-case NEXT scenario will occur in the central office since lines branch out closer to the customer.

Most HDSL studies model crosstalk as stationary gaussian noise with a power spectrum given by

$$|H_{NEXT}(f)|^2 = Kf^{3/2} \tag{3.4}$$

where $K=10^{-13}$ is a constant and $H_{NEXT}(f)$ is the frequency response of the NEXT co-channel coupling. An important factor not considered in such a model is the relative phase among the various interferers. Practical loop-plant studies have indicated that the crosstalk statistics can vary under different synchronization conditions. The crosstalk statistics can be cyclostationary if the interferers are in phase or if the interference is dominated by a few interferers [38]. Cyclostationary processes are those where the inherent physical phenomena give rise to periodicities and consequently the appropriate probablistic models exhibit periodically time-varying parameters. The case of interference being dominated by a few interferers has been found to occur in many practical situations in [36]. The degree of cyclostationarity is governed by the amount of synchronization achievable within the loop plant [33].

Interference from digital signals are in general cyclostationary, but if the relative phase of multiple interferers is randomized, then the resulting crosstalk has stationary statistics [34]. This fact has been revealed in practical crosstalk measurements where the cyclostationarity is manifested as varying crosstalk power within a symbol period. When the interference is stationary the power is constant in a symbol period.

One approach in simulating the crosstalk with all the synchronization effects is to measure the crosstalk impulse response in a typical cable pair as was done in [36]. Since access to such a facility was not available, we used simulation models which could simulate the extreme cases of synchronization.

A worst-case crosstalk model for a single interferer was obtained from [18] and is given as

$$H_{NEXT1}(f) = K_1 f^{3/4} \tag{3.5}$$

where $K_1 = 10^{-7}$ and $H_{NEXT1}(f)$ is the coupled frequency response of a single interferer. This is modeled using an $f^{3/4}$ filter designed using [35] and the effects of the transformer and hybrid are then included. The impulse response of the single interferer obtained using this method is shown in Fig. 3.8. The use of this single interferer for

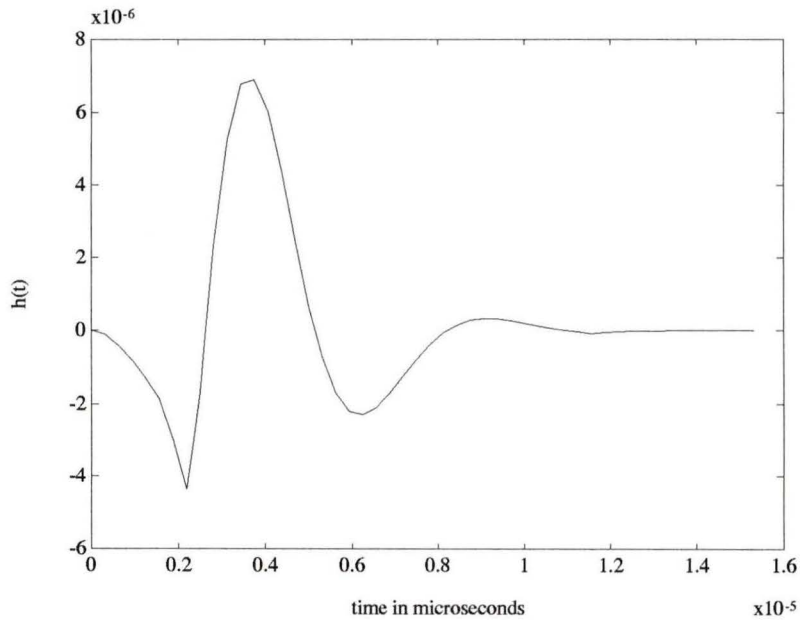

Figure 3.8 Worst-case crosstalk impulse response used in HDSL equalizer simulation

modeling the crosstalk under different synchronization conditions will be outlined in a later section.

3.5 ISI and Crosstalk Suppression using FSE

In this section we review the theory presented in [32][33], which can be used in achieving satisfactory performance levels in an HDSL equalizer. The relevance of the theory to the HDSL scenario is explained and helps in devising a successful scheme for the HDSL equalizer.

The goal of an equalizer is to suppress ISI and crosstalk without enhancing noise at the input. This enables reliable detection of the transmitted sequence.

Consider the model shown in Fig. 3.9 where the channel output along with the crosstalk is shown [32].

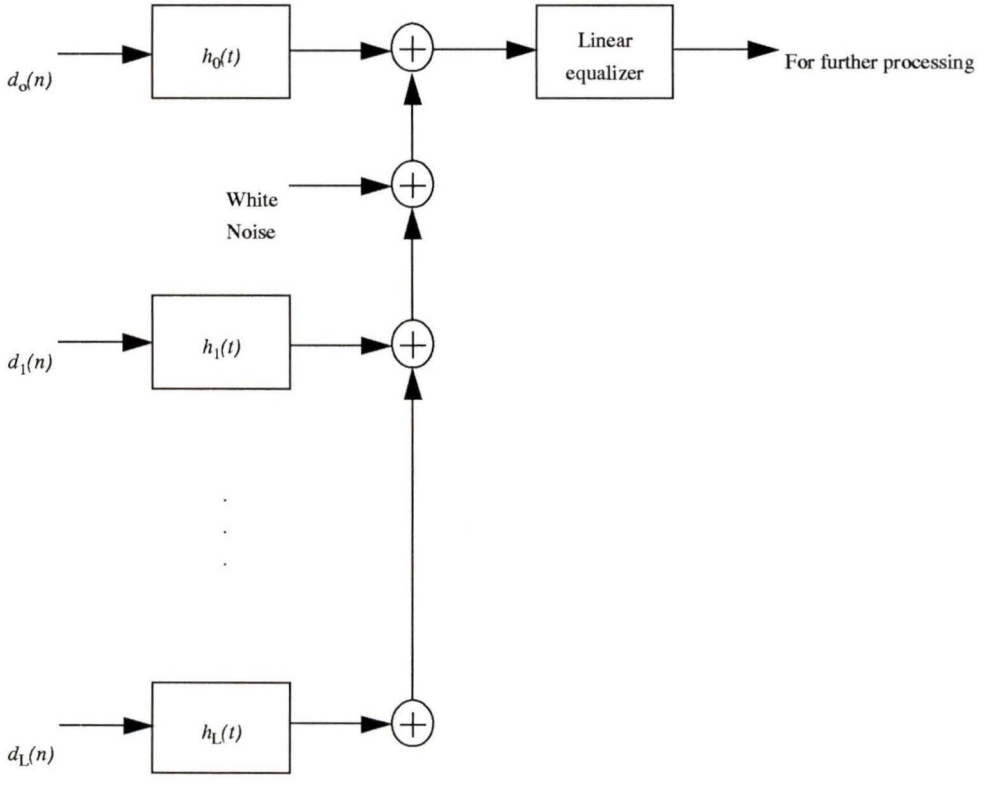

Figure 3.9 Linear equalizer operation in a cyclostationary crosstalk environment

For this model let us define two sets L_0 and L_1 as

$L_0 = \{0, 1, 2, 3, \ldots, L\}$ and $L_1 = \{1, 2, 3, \ldots, L\}$ where L is the number of interferers in the cable. Let $h_0(t)$ be the impulse response of the signal channel and let $h_i(t)$ where $i = 1, 2, \ldots, L$ be the impulse responses of the interferers (co-channels) in the cable. Let $r_l(t)$ be the impulse response of the linear equalizer as shown in Fig. 3.9.

The equalized combined channel or combined co-channels can be defined as

$$h_{ic}(t) = h_i(t) \otimes r_l(t) \qquad (i \in L_0) \tag{3.6}$$

where $\otimes$ denotes convolution. A frequency-domain equivalent of (3.6) can be written as

$$H_{ic}(f) = H_i(f) R_l(f) \qquad (i \in L_0) \tag{3.7}$$

The time-domain condition for zero ISI can be written as

$$h_{0c}(nT) = \delta(n) \tag{3.8}$$

and the time-domain condition for zero co-channel interference can be written as

$$h_{ic}(nT) = 0 \qquad (i \in L_1) \tag{3.9}$$

These conditions can be illustrated as in Fig. 3.10.

The time-domain condition for zero ISI and zero co-channel interference can be expressed in the frequency domain as

$$\frac{1}{T} \sum_{l=-\infty}^{\infty} H_{ic}\left(f + \frac{l}{T}\right) = \delta(i) \qquad (i \in L_0) \tag{3.10}$$

Substituting (3.7) in (3.10) we obtain

$$\frac{1}{T} \sum_{k=-\infty}^{\infty} H_i\left(f + \frac{k}{T}\right) R_l\left(f + \frac{k}{T}\right) = \delta(i) \qquad (i \in L_0) \tag{3.11}$$

If $H_i(f)$ and $R_l(f)$ are strictly bandlimited [32] to 1/(2T) then (3.11) reduces to

$$H_i(f) R_l(f) = T\delta(i) \qquad \left(0 < f < \frac{1}{2T}\right) \quad (i \in L_0) \tag{3.12}$$

For the likelihood of a solution to exist, the number of equations must be less than or equal to the number of unknowns. Since there is only one unknown ($R_1(f)$) and L+1 equations we require that $L+1<=1$. Therefore, L is less than or equal to 0. This means that no interferers can be suppressed.

If the combined channels and combined co-channels are strictly bandlimited to 2/(2T), then (3.11) reduces to

$$H_i(f-\frac{1}{T})R_l(f-\frac{1}{T})+H_i(f)R_l(f) = T\delta(i) \qquad (i \in L_0) \quad (0<f<\frac{1}{2T}) \tag{3.13}$$

and because of the bandwidth condition, there are two unknowns ($R_1(f)$, $R_1(f-1/T)$). As a result, we have $L+1<=2$ which makes L less than or equal to 1. Therefore, one interferer can be suppressed.

In general this result can be extended as follows. If the channel and co-channel are strictly bandlimited to $K/(2T)$ and if there are $N=L+1$ independent data streams then a likely solution for (3.11) will exist when the number of independent data

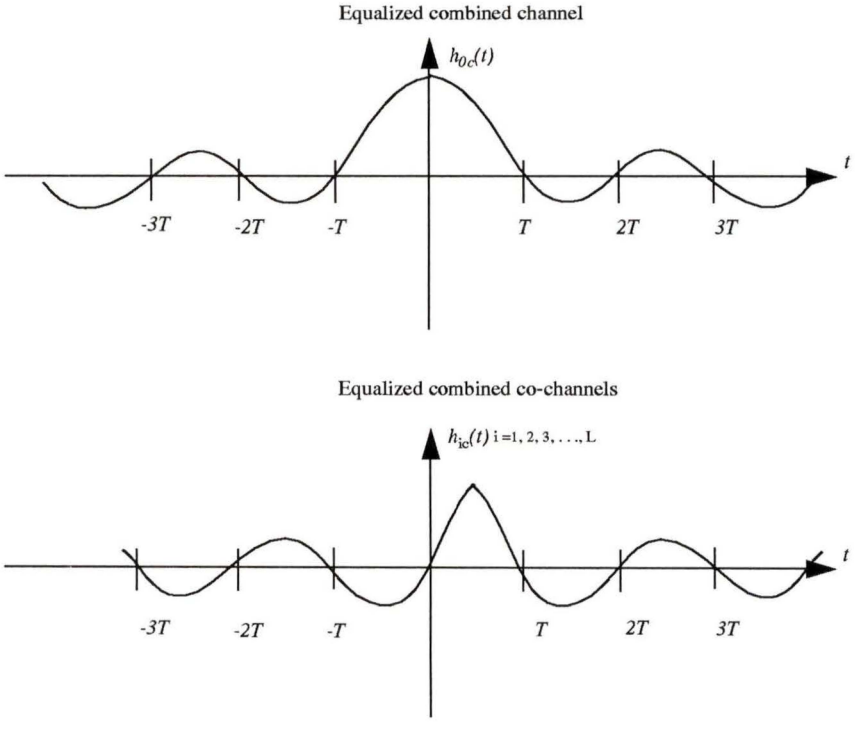

Figure 3.10 Generalized zero-forcing condition for the combined channel and combined co-channels

streams is less than or equal to the parameter (K) controlling the bandwidth, i.e.,

$$N \leq K \tag{3.14}$$

3.6 Cyclostationary Crosstalk Suppression for HDSL

The preceding result can be used for realizing crosstalk suppression in the HDSL equalizer. The gist of the idea is that cyclostationary crosstalk can be suppressed by means of increased bandwidth in the combined channel and co-channels. Increased bandwidth means that the forward equalizer has to be proportionately fractionally tap-spaced, e.g., for a bandwidth of $N/2T$, the equalizer has to be tap-spaced at T/N.

Thus with a T/N tap-spaced equalizer (assuming that the bandwidth criteria is met), N-1 cyclostationary interferers can be suppressed along with ISI. However, there could be several problems with increasing the bandwidth in the HDSL system (increasing white noise, vulnerability to impulse noise [6], compatibility with other services in the loop plant etc.). Most research groups which represent HDSL vendors have prescribed to using a 200-kHz cutoff transmit and receive filter and, as a result, there would be very little signal energy above 400 kHz [39]. Given this, crosstalk can be effectively suppressed under two conditions: 1) All the interferers are synchronized, thus effectively resulting in one interferer to suppress; and 2) use a T/2-spaced equalizer for suppressing this single cyclostationary interferer along with ISI. This is the basis for our equalizer simulations in the following sections.

3.7 Simulation Description

The channel and crosstalk modelling have been outlined. These responses are sampled at several times the symbol rate and are used for testing the effect of sampling phase on the equalizer performance. All the simulations were performed in MATLAB^{TM}.

3.7.1 Signal generation at the receiver input

The transmitted sequence is 2B1Q (4 levels) and is normalized to have unit power. For obtaining a higher rate data signal, say m times the symbol rate, m-1 zeros are inserted between adjacent symbols. This sequence is then convolved with the higher-rate sampled channel to obtain the signal output from the channel.

3.7.2 NEXT Generation

As mentioned earlier, we use a single worst-case NEXT response to simulate the effects of up to 49 interferers. This is based on the fact that the measured crosstalk responses from different cable pairs showed very little difference in practical measurements [36]. Our NEXT modeling concentrates on two extreme cases: NEXT from completely synchronized interferers or NEXT from interferers with random phase which appears as stationary noise.

A general procedure for obtaining crosstalk from multiple interferers is to pass independent data sequences through the crosstalk filters and sum them up at the receiver. Since the crosstalk responses are similar, synchronization masks the fact that there are different interferers [38]. This means that one can use a single interferer and a data sequence with sufficient power to simulate crosstalk from various numbers of synchronized interferers. The variance of this single crosstalk input generator is equal to α, the number of active interferers. This input sequence is then converted into a higher rate sequence by zero padding as outlined earlier. The variation of the cyclostationary crosstalk power in a symbol period is illustrated in Fig. 3.11.

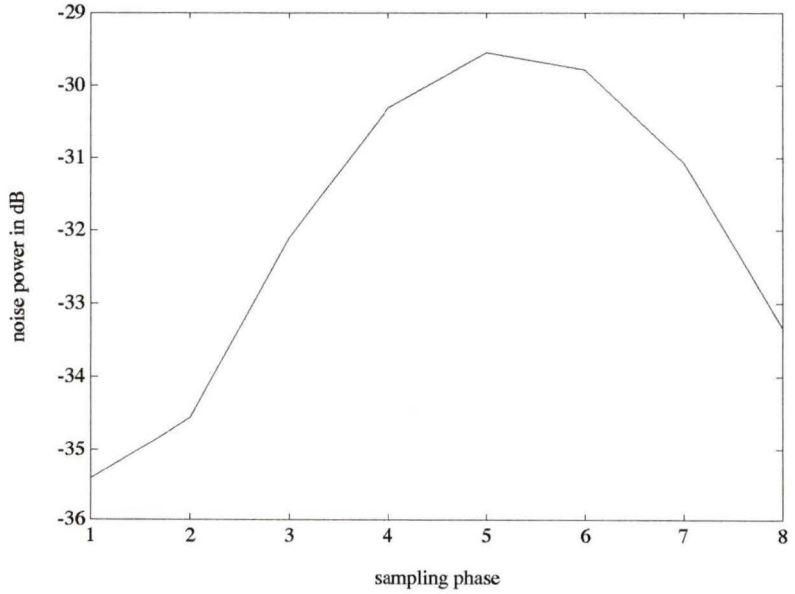

Figure 3.11 Crosstalk power variation from a single interferer in a symbol period

For stationary noise, all the m input samples in a symbol period have white gaussian statistics and the power of this sequence is given by α/m (the number of interferers divided by the sampling rate factor). The input sequences in both cases (synchro-

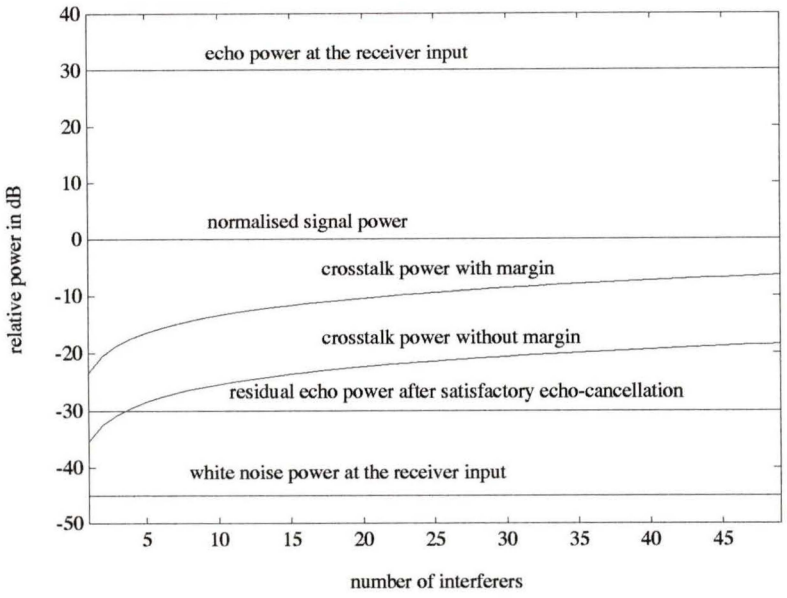

Figure 3.12 Relative power level of signals at the equalizer input

nized, and stationary case) are then passed through the crosstalk filters in (3.5) to obtain the crosstalk output. The relative power levels of the different signals at the input of the receiver is shown in Fig. 3.12 for a 13-kft 24-gauge loop for increasing numbers of interferers.

White noise of adequate power [37] is also added to the above mentioned signals at the input of the receiver. These signals are then filtered by a lowpass filter before processing by the equalizer. The input signal power of the equalizer is normalized to have unit power for comparison with other equalizer simulations [32]. Impulse noise can also be a minor source of distortion at the receiver but lack of a appropriate model makes it difficult to include it in the simulations.

3.8 Equalizer Performance Evaluation

A recommended margin for NEXT in the HDSL equalizer studies is 12 dB [32] and this is included in the NEXT model. The ultimate performance measure of the equalizer is the bit-error rate which is prescribed to be 10^{-7}. Testing this bit-error rate measure by means of simulations using limited computing resources would take an enormous amount of time. Hence the MSE is used as a measure of performance for the equalizer. A typical performance measure that has been used before is a 21.5-dB MSE assuming unit data variance [39]. In our simulations, we will use this perfor-

mance measure while evaluating the equalizers. In a later section, the decision-directed equalizer's performance will be measured in terms of the symbol-error, although for comparatively short sequences.

3.9 Adaptive Algorithm

The LMS algorithm was the first choice for adapting the forward and feedback filters in the DFE. The reasons for choosing the LMS algorithm were made clear in the preceding chapter. However, unlike the echo canceler, the input to the forward equalizer is a symbol sequence and as a result the input could be ill-conditioned. The other choices were the RLS and FRLS algorithms which involve a high degree of numerical complexity and are not guaranteed to be numerically stable.

If $\boldsymbol{r}_f$ and $\boldsymbol{r}_d$ are the vectors of forward and feedback filter coefficients respectively, then the LMS adaptation algorithm used in the following simulations is

$$\boldsymbol{r}_f(n+1) = \boldsymbol{r}_f(n+1) + \mu e(n)\,\boldsymbol{u}_f(n) \tag{3.15}$$

$$\boldsymbol{r}_d(n+1) = \boldsymbol{r}_d(n+1) + \mu e(n)\,\boldsymbol{u}_d(n) \tag{3.16}$$

where

$$e(n) = d(n) - y(n) \tag{3.17}$$

$$y(n) = \boldsymbol{r}_f^t(n)\,\boldsymbol{u}_f(n) + \boldsymbol{r}_d^t(n)\,\boldsymbol{u}_d(n) \tag{3.18}$$

and μ is the convergence factor used in the simulations.

3.10 Simulation Results and Discussion

3.10.1 Influence of sampling phase

The theoretical results presented in [32] suggest that a T/2 equalizer should be able to suppress one interferer and ISI. Finite-length MMSE equalizers can only approach these results. In our simulations we will only explore the completely synchronized and stationary crosstalk scenarios for T/2 and T-spaced equalizers.

The influence of sampling phase on the equalizer performance is important as it may simplify the timing recovery scheme used in the receiver. FSEs have obviously better performance with regard to sampling phase whereas SSEs are more sensitive with respect to the sampling phase.

The performance of the T/2 FSE and the SSE under synchronized and stationary crosstalk conditions with respect to the sampling phase is illustrated in Fig. 3.13.

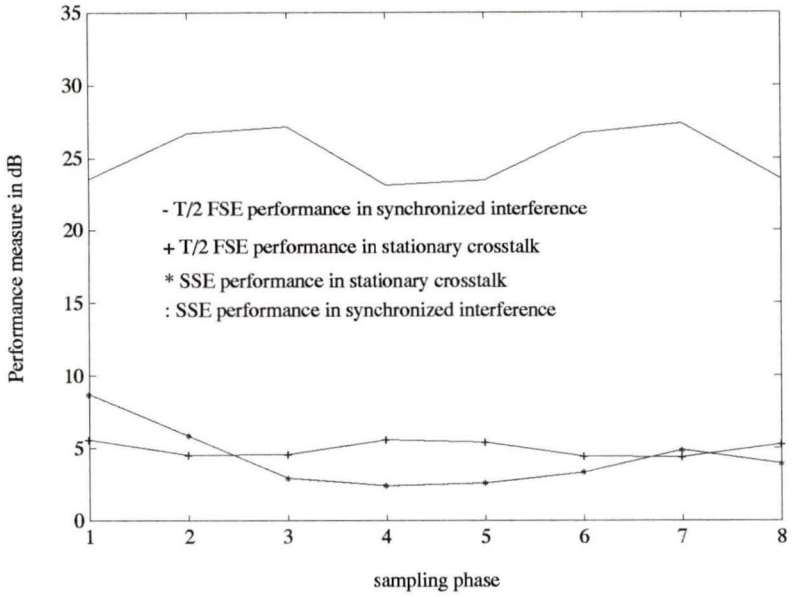

Figure 3.13 Performance of SSE and T/2 FSE under different crosstalk conditions with respect to sampling phase

In this experiment, the crosstalk was simulated to be from 49 interferers. The LMS algorithm was used in the simulations running for 10 ensembles each with 200,000 iterations and with a convergence factor $\mu = 0.005$. The MSE over the last 1000 iterations were averaged and this mean was used as the performance measure in the simulations. The plot shows that the T/2 FSE under cyclostationary crosstalk conditions is far superior than the one working under stationary noise conditions or either SSE scenario. The equalizer was used in a training mode only. The delay was made nearly optimal by trial and error, and the orders of the forward and feedback filters are (11, 50) for the SSE and (21, 50) for the T/2 FSE, respectively. These were also found after sufficient experimentation with various orders for the filters. The SSE was tested for higher than reported orders but the performance showed no significant improvement, which is as predicted from the theoretical observations in the earlier chapter. The forward filter orders for the FSE and SSE were chosen to have the same temporal span in the impulse response of the filters. Since the T/2 FSE was found to work satisfactorily irrespective of the sampling phase, we will use one particular phase for most of the other simulations. The best phases for the other cases will be used for comparison.

3.10.2 Equalizer performance with different numbers of interferers

The performance of the equalizer with varying numbers of interferers is illustrated in Fig. 3.14. In this simulation, the performance of the equalizer with various numbers

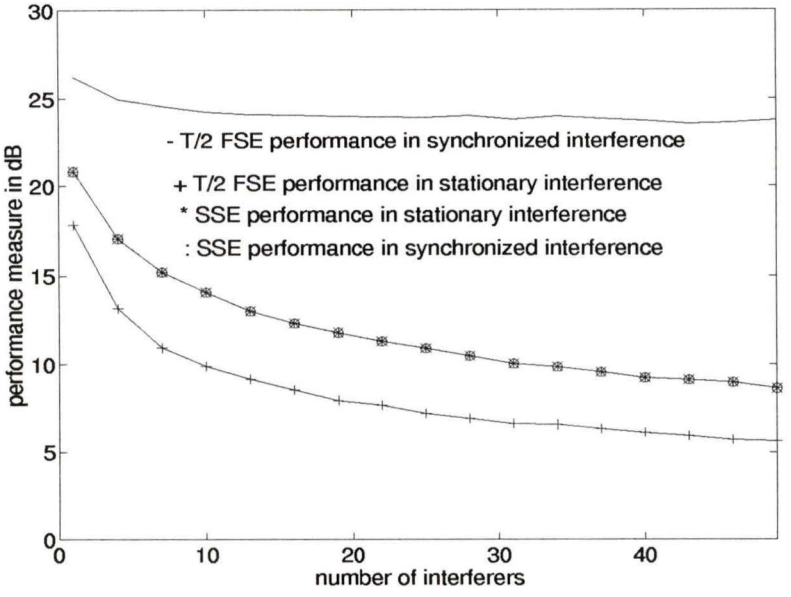

Figure 3.14 Performance of equalizers in different crosstalk environments and with varying numbers of interferers

of interferers α was monitored using the MSE after 200,000 iterations and 10 ensembles for each α. The LMS algorithm was used in the simulations. The SSE's performance in either crosstalk conditions does not differ and hence the performance difference among the two is not visible.

The T/2 FSE's performance under cyclostationary crosstalk conditions does not vary much with increasing numbers of interferers. Since we have a synchronized loop plant, and since the crosstalk response from the various cables are assumed similar, the equalizer's task is the suppression of this response. The only change when increasing the numbers of interferers is the increasing data variance, which has very minimal effect. The other cases illustrated in the figure show performance degradation which increases with the number of interferers.

The converged tap coefficients of the forward and feedback filter under cyclostationary crosstalk conditions for 1 interferer and 49 interferers are shown in Figs. 3.15 and 3.16. It can be seen that the coefficients are similar. This implies that, with synchronized interferers, the equalizer is somewhat insensitive to the actual number

of interferers.

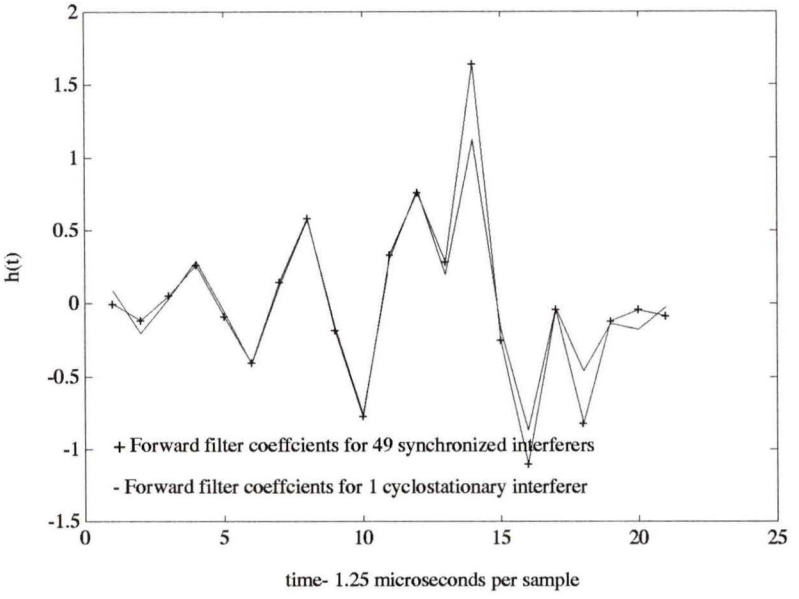

Figure 3.15 Comparison of converged forward filter coefficients of a T/2 FSE with different numbers of synchronized interferers.

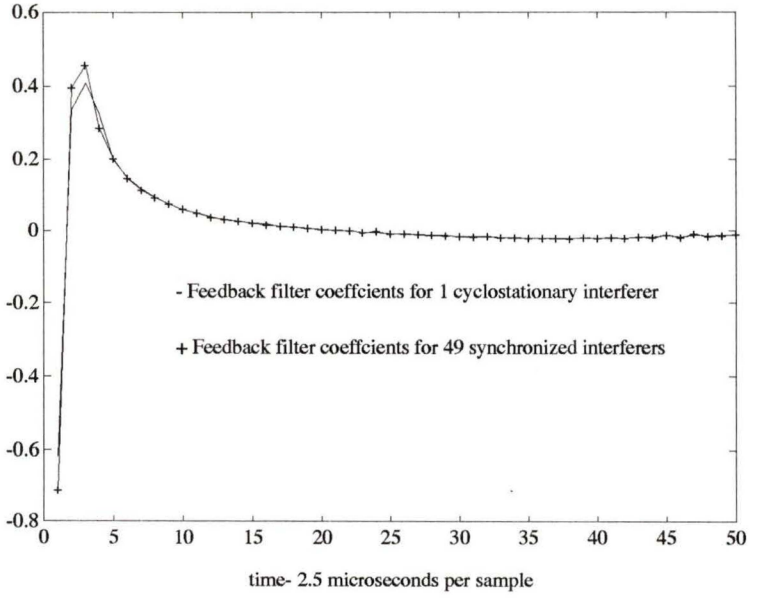

Figure 3.16 Comparison of converged feedback filter coefficients of a T/2 FSE with different numbers of synchronized interferers

3.11 Decision-Directed Equalization

In decision-directed equalization, the equalizer operates in a real-world scenario where, after sufficient training, it uses its hard-limited output as the desired response. This is illustrated for a DFE in Fig. 3.17. The purpose of this section is to realisti-

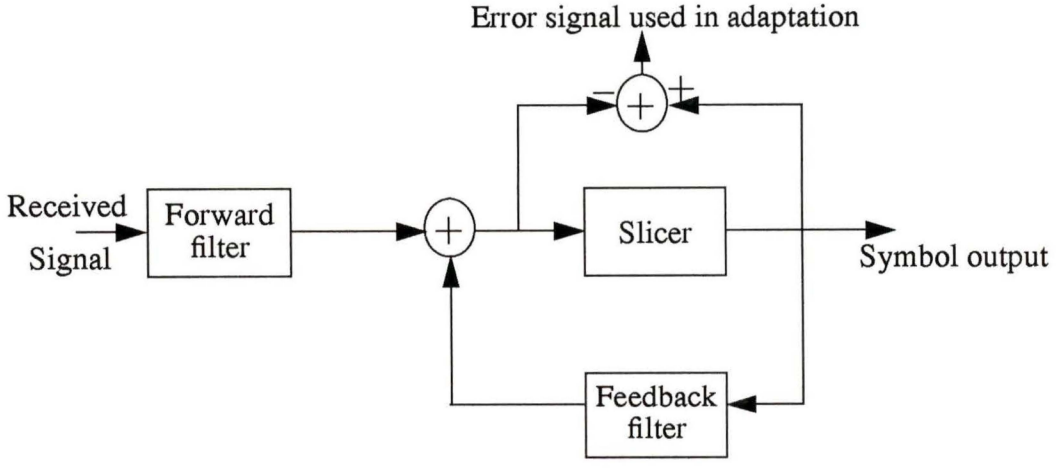

Figure 3.17 Decision directed equalizer operation

cally estimate the training time needed for an HDSL equalizer. The decision-directed equalizer (DDE) was simulated for different training lengths using the LMS algorithm. In this experiment, the average symbol-errors for different training lengths is measured. The simulation was run for 50,000 iterations and the average symbol-error was calculated from the total symbol-errors in 10 ensembles. This is shown in Fig. 3.18 where the average symbol errors for different training lengths is shown. The NEXT in this case was synchronized and was assumed to be from 49 interferers. The experiment indicates that under synchronized noise conditions, a worst-case training length of 20, 000 iterations might be required in HDSL i.e., with a symbol rate of 400 ksymbols/s, the training period required is 50 ms.

3.12 Effect of Highpass Filter in the Equalizer

In the last chapter, a highpass filtering technique for reducing the complexity of the echo canceler was proposed and was found to work successfully. Since the highpass filter was in the receiver path, the received far-end signal is also highpass filtered by

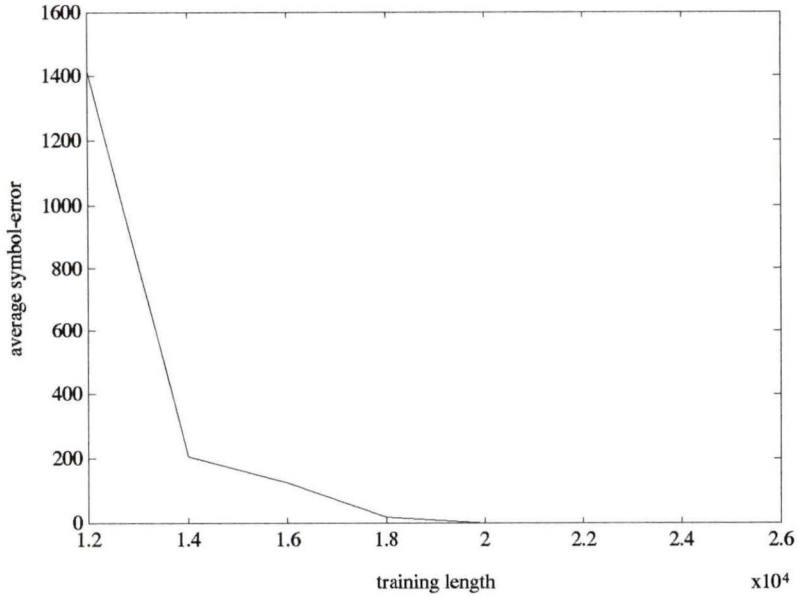

Figure 3.18 Performance of decision-directed equalizer under different training lengths

this technique. The effectiveness of this technique for echo cancellation was demonstrated, but the performance of the equalizer with this additional highpass filter in the signal path must be evaluated.

In this experiment, we used a 4th-order Butterworth highpass filter with a 25-kHz cutoff frequency since this filter was shown to have resulted in good performance for the echo cancelers. To achieve the performance of 21.5 dB (outlined earlier), the forward filter order needed to be increased from 21 to 31 taps, but the feedback filter order can be reduced from 50 to 30 taps. The simulated performance of the DFE with a receive highpass filter is shown in Fig. 3.19. The performance shows that highpass filters which are used for reducing the echo-canceler complexity will not degrade the equalizer performance, provided the number of forward filter taps is suitably adjusted. The forward filter order needed might have to be increased by a few taps as in our case, but the feedback filter order can be reduced. The benefit of this technique might be more beneficial in the case of hybrid transformers with larger primary inductances which cause long channel (and echo) tails since substantial reduction in the feedback equalizer complexity can also be achieved.

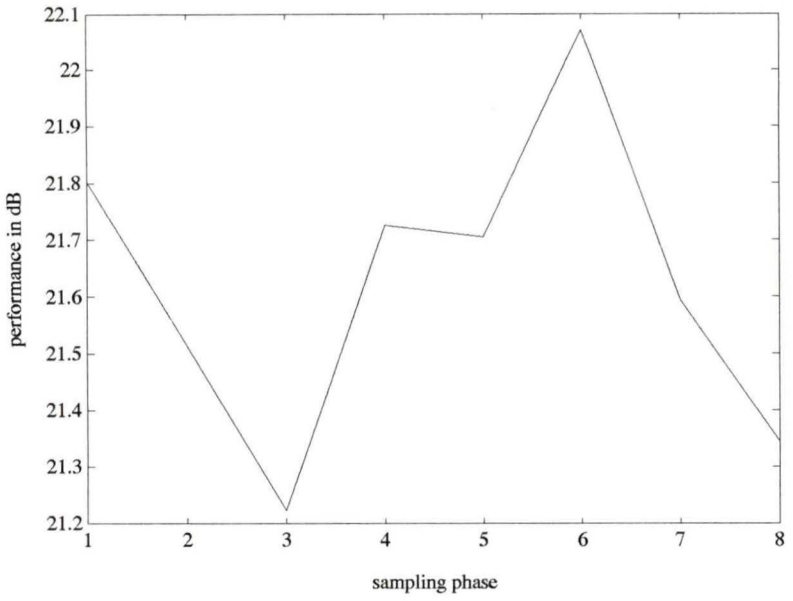

Figure 3.19 Performance of DFE with a highpass receive filter in the signal path

3.13 Conclusion

This chapter dealt with HDSL equalization. Since NEXT is the main obstacle in limiting the range of the HDSL system, primary attention is devoted to the study of the NEXT. Different synchronization conditions in the central office can result in different NEXT statistics and this was explained in detail.

An important theoretical result which was used in this chapter was originally derived in [33], where the advantages of increased bandwidths in suppressing cyclostationary crosstalk was presented. This was investigated for the HDSL case and a FSE (T/2) which operates in a synchronized crosstalk environment was found to be needed to achieve the performance requirements in HDSL. An interpretation based on this result for the HDSL equalization case was presented, and was used in the simulations. Symbol by symbol simulations were presented using the LMS algorithm and the performance of the T/2 FSE with a 13-kft 24-gauge line were found to be satisfactory with a 12 dB NEXT margin. The performance variations as a function of number of interferers was illustrated and training lengths for a practical DFE working in HDSL were presented.

The highpass filtering technique which was introduced for reducing the com-

plexity of the echo canceler was also introduced into the far-end signal path, as for a practical transceiver configuration, the highpass filter will also be in the received signal path. Hence this was introduced in the equalizer simulations and the satisfactory equalizer performance was achieved with an increase in the forward-filter length and a reduced number of feedback coefficients.

Chapter 4

Conclusions and Suggestions for Further Work

4.1 Conclusions

The main goal of this work was to examine the performance of echo cancelers and equalizers in the HDSL environment. The performance of these two elements satisfying prescribed standards was studied using a detailed simulation environment.

The echo-path model was built using a transformer which helps in complexity reduction and was used in testing the echo canceler. The length of the echo canceler needed to achieve the performance specifications was obtained for three worst-case loops and the results can be considered as a worst-case estimate of the echo-canceler order needed in a practical HDSL system. Echo-canceler order reduction can be achieved using transformers with reduced primary inductance values. The echo canceler might have to interface in a certain fashion with the equalizer in the transceiver and one particular scenario was investigated. Techniques proposed in the literature for reducing the complexity in echo cancelers were tested, and some comparatory comments between the highpass filtering technique and these techniques have been presented.

The NEXT was seen as the limiting factor in the HDSL system implementation and along with ISI forms a strong impediment for reliable data transmission. The NEXT environment is clearly outlined for different synchronization conditions and the relative power of the signals in the loop plant is illustrated. A recently proposed concept in cyclostationary crosstalk suppression has been explained with relevance to HDSL equalization. Simulations of the HDSL equalizer under different NEXT conditions have been performed. Satisfactory performance is shown to be achieved only in the case of com-

plete synchronization in the loop plant.

The performance of the decision-directed equalizer has been presented and the highpass filtering technique proposed in the second chapter was used in the signal path to test the performance of the equalizer. Except for a slight increase in complexity, the performance of the equalizer was shown to be satisfactory.

4.2 Suggestions for Further Work

This thesis presented the HDSL echo canceler and equalizer acting separately. In an HDSL transceiver, however, these two elements may have to be implemented in a single chip and there could be several issues which could arise in the joint working of the equalizer and echo canceler.

Theoretical MMSE calculations favor the forward filter [18] to be present before the equalizer, but this could become a problem for the crosstalk suppression used in this thesis. This is because of the fact that the echo from the near-end data transmitter is a cyclostationary signal, and has considerably more power than crosstalk (and of course the far-end signal). Hence the forward filter might have problems with the crosstalk suppression. Practical adaptation studies favor the echo cancellation to be done ahead of the equalization [22]. In this case the echo canceler has to be interleaved as outlined in the chapter 2. Even in this case, when the NEXT is low, the residual echo power is more as shown in Fig. 3.12 and could result in poor NEXT suppression in the forward filter.

These issues could be investigated in detail and a viable configuration exploiting the NEXT suppression properties of the FSE could be used in a practical HDSL transceiver. As mentioned earlier, impulse noise has not been included in the model as in many other HDSL studies [43], and needs to be investigated in detail using an appropriate model. Detailed information about interference from other services in the subscriber loop plant can also help in simplification of the forward equalizer. The use of the highpass filter in the receiver path in overcoming some of this interference could also be investigated.

References

[1] B. R. Saltzberg, R. Hsing, J. M. Cioffi, and D. W. Lin, "Guest Editorial", *IEEE J. Select. Areas. Commun.*, vol. 9, pp. 761-764, Aug. 1991.

[2] H. Cravis and T. V. Crater, "Engineering of T1 carrier system repeatered lines," *Bell Syst. Tech. J.*, vol. 42, pp. 431-486, Mar. 1963.

[3] J. W. Lechleider, "High bit rate digital subscriber lines: a review of HDSL progress," *IEEE J. Select. Areas. Commun.*, vol. 9, pp. 769-784, Aug. 1991.

[4] D. W. Lin and M.L.Liou, "A tutorial on digital subscriber line transceiver for ISDN," *Proc. IEEE Symp. Circuits Syst*, pp. 839-846, June 1988.

[5] D. T. Huang and C. F. Valenti, " Digital subscriber lines: Network considerations for ISDN basic access standard," *Proc. IEEE*, vol. 79, pp. 125-144, Feb. 1991.

[6] J. J. Werner, "The HDSL environment," *IEEE J. Select. Areas Commun.*, vol. 9, pp. 785-800, Aug. 1991.

[7] R. Komiya, K. Yoshida, and N. Tamaki, "The loop coverage comparison between TCM and echo-canceler under various noise conditions," *IEEE Trans. Commun.*, Vol. 34, pp. 1058-1067, Nov. 1986.

[8] C. A. Belfiore and J. H. Park, "Decision Feedback Equalization," *Proc. IEEE*, vol. 67, pp. 1143-1156, Aug. 1979.

[9] S. U. H. Qureshi, "Adaptive Equalization," *Proc. IEEE*, vol. 73, pp. 1349-1387, Sep. 1985.

[10] D. G. Messerschmitt, "Echo cancellation in speech and data transmission," *IEEE J. Select. Areas Commun*, vol. 2, pp. 283-297, Mar. 1984.

[11] M. Sondhi and D. A. Berkley, "Silencing echos on the telephone network," *Proc. IEEE*, vol. 68, pp. 948-963, Aug. 1980.

[12] D. L. Waring, J. W. Lechleider, and T.R. Hsing, "Digital subscriber line technology facilitates a graceful transition from copper to fiber," *IEEE Commun. Mag.*, vol. 29, pp. 96-104, Mar. 1991.

[13] W. Y. Chen, J. L. Dixon, and D. L. Waring, "High bit rate digital subscriber line echo cancellation," *IEEE J. Select. Areas Commun.*, vol 9, pp. 848-860, Aug. 1991.

[14] "Study of the feasibility and advisability of digital subscriber lines operating at rates substantially in excess of the basic access rate," ANSI T1E1.4, Aug. 1991.

[15] G. S. Moschytz and S. V. Ahamed, "Transhybrid loss with RC balance circuits for primary-rate ISDN transmission systems," *IEEE J. Select. Areas Commun.*, vol. 9, pp. 951-959, August 1991.

[16] Bell Telephone Laboratories, *Transmission Systems for Communications*, 5th ed., 1982.

[17] A. Abousaada, "*Echo Tail Canceller Based on AIFIR Filtering*," M.S. thesis, Ottawa-Carleton Institute for Electrical Engineering, Jan. 1990.

[18] D. W. Lin, "Minimum mean-square echo cancellation and equalization for digital subscriber line transmission: Parts I and II, " *IEEE Trans. Commun.*, vol. 38, pp. 31-45, Jan. 1990.

[19] S. Haykin, *Adaptive Filter Theory*, Second Edition, Prentice Hall, New Jersey, 1991.

[20] G. Young, "Reduced complexity decision feedback equalization for digital subscriber loops," *IEEE J. Select. Areas Commun.*, vol. 9, pp. 810-816, Aug. 1991.

[21] A. Antoniou, *Digital Filters: Analysis, Design, and Applications*, 2nd ed., McGraw-Hill, New York, 1993.

[22] D. D. Falconer and K. H. Mueller, "Adaptive echo cancellation/ AGC structures for two-wire full duplex data transmission," *Bell Syst. Tech. J.*, vol. 58, pp. 1593-1616, Sep. 1979.

[23] G. W. Davidson, and D. D. Falconer, "Reduced complexity echo cancellation using orthonormal functions," *IEEE Trans. Circ. Syst.*, vol. 38, pp. 20-28, Jan. 1991.

[24] A. Abousada, T. Aboulnasr, and W. Steenaart, "An echo tail canceller based on adaptive interpolated FIR filtering," *IEEE Trans. Circ. Syst.*, vol. 39, pp. 409-416, July 1992.

[25] Y. Neuvo, C. Y. Dong, and S. K. Mitra, "Interpolated finite impulse response filters," *IEEE Trans. Acoust., Speech, Signal Processing*, vol. 32, pp. 563-570, June 1984.

[26] N. J. Lynch-Aird, "Review and analytical comparison of recursive and nonrecursive equalization techniques for PAM transmission systems," *IEEE J. Select. Areas Commun.*, vol. 9, pp. 830-838, Aug. 1991.

[27] G. Ungerboeck, "Fractional tap-spacing equalizer and consequences for clock recovery in data modems," *IEEE Trans. on Commun.*, vol. 24, pp. 856-864, Aug. 1976.

[28] E. A. Lee and D. G. Messerschmitt, *Digital Communication*, Kluwer Academic, 1988.

[29] J. A. C. Bingham, *The Theory and Practice of Modem Design*, Wiley, 1988.

[30] J. G. Proakis, *Digital Communications*, McGraw-Hill Inc., 1983.

[31] T. Bartee, "*ISDN, DECnet, and SNA Communications,*", Howard Sams, 1988.

[32] B. R. Petersen, "*Equalization in Cyclostationary Interference,*" Ph.D. thesis, Department of Systems and Computer Engineering, Carleton university, Ottawa, Jan. 1992.

[33] B. R. Petersen and D. D. Falconer, "Minimum mean-square equalization in cyclostationary and stationary interference-analysis and subscriber-line calculations," *IEEE J. Select. Areas Commun.*, vol. 9, pp. 931-941, Aug. 1991.

[34] W. A. Gardner, *Introduction to Random Processes with Applications to Signals and Systems,* McGraw-Hill, 2nd ed., 1990.

[35] D. J. Shpak and A. Antoniou, "A generalized Remez method for the design of FIR digital filters," *IEEE Trans. Circ. Syst.*, vol. 37, pp. 161-174, Feb. 1990.

[36] A. Fung, L. S. Lee, and D. D. Falconer, "A facility for near end crosstalk measurements on ISDN subscriber loops," *Conf. Rec. IEEE Globecom 89*, vol. 3, pp.1592-1596, Nov. 1989.

[37] M. Abdulrahman, "*Decision-Feedback Equalization with Cyclostationary Interference for DSL,*" Master's thesis, Department of Systems and Computer Engineering, Carleton university, Ottawa, June 1989.

[38] M. Abdulrahman and D. D. Falconer, "Cyclostationary crosstalk suppression by decision feedback equalization on digital subscriber loops," *IEEE J. Select. Areas Commun.*, vol. 10, pp. 640-649,April 1992.

[39] H. Samueli, B. Daneshrad, R. B. Joshi, B. C. Wong, and H. T. Nicholas, III, "A 64 tap CMOS echo canceller/decision feedback equalizer for 2B1Q HDSL transceivers," *IEEE J. Select. Areas Commun.*, vol. 9, pp. 839-847, Aug. 1991.

[40] M. Abdulrahman, "private communication", Carleton University, Ottawa, August 1992.

[41] B. R. Petersen, "private communication", IBM, Zurich, Nov. 1992.

[42] P. Mohanraj, "*Investigation of Coding and Equalization Algorithms and VLSI Architectures for a High Bit-rate Digital Subscriber Loop System,*" Ph.D. thesis, Department of Electronics, Carleton University, Ottawa, Dec. 1990.

[43] "Special issue on high bit-rate digital subscriber lines," *IEEE J. Sel. Areas Commun.*, vol. 9, Aug. 1991.

[44] J. C. Campbell, A. J. Gibbs, "The cyclostationary nature of crosstalk interference from digital signals in multipair cabel-Part I: Fundamentals and Part II: Applications and furhter results," *IEEE Trans. on Commun.*, vol. 31, pp. 629-649, May 1983.

Appendices

Appendix A

Echo-tail analysis

A.1 Dominant pole in the echo-path transfer function

In this appendix, we derive the approximate pole positions of the echo path. This is done by using standard assumptions for the input impedance of the cable. The information about the dominant pole position, which causes the long echo tails, can then be cancelled suitably. From (2.1), the echo-path transfer function is given as

$$H(s) = \frac{Z_{bal}}{Z_o + Z_{bal}} - \frac{Z_{in}}{Z_o + Z_{in}} \tag{A.1}$$

where

Z_{bal} = Balance impedance (110 ohms)

Z_o = Series impedance (110 ohms)

Z_{in} = Input impedance of the loop looking in through the transformer.

The values of Z_{bal} and Z_o were approximated using the standard nominal value of 110 ohms. Z_{in} can be calculated using the transformer equivalent circuit shown in Fig. 2.3. The average cable input impedance of 110 ohms, as suggested by calculations in [16], is used and cable input impedances of some of the echo paths are plotted in Fig. A.1. Using Z_{in}, the dominant echo-path poles can be calculated by representing the echo-path transfer function as

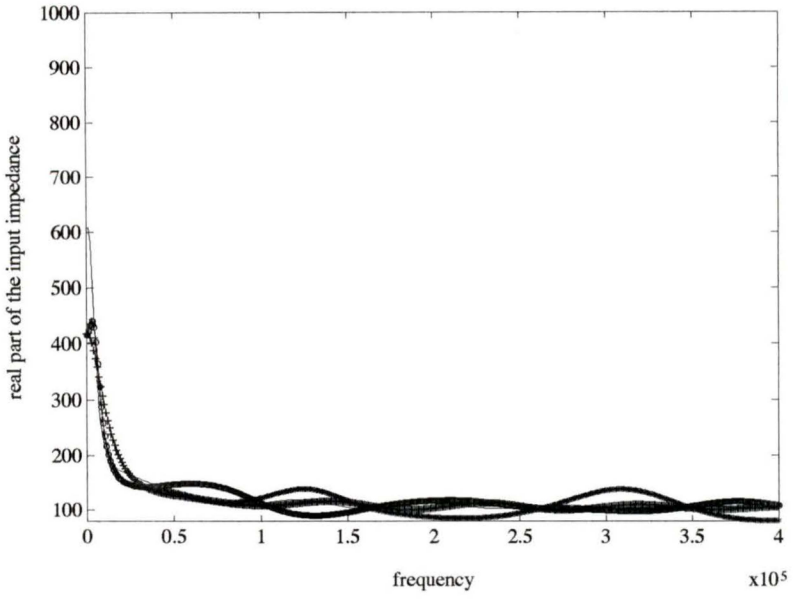

Figure A.1. Variation of cable input impedance with frequency

$$H(s) = \frac{N(s)}{D(s)} \tag{A.2}$$

The poles in the transfer function are obtained by solving the equation

$$D(s) = 0 \tag{A.3}$$

Two real poles were obtained by solving this second-order equation and one of the poles was found to be much closer to the imaginary axis than the other one. The pole positions are given by

S_1=-0.0002 e8

S_2=-1.0942 e8

S_1 is the dominant pole and the corresponding frequency position is 2.9 kHz.

VITA

Surname: Subramanian Given Names: Srikanth

Place of Birth: Nagercoil Date of Birth: 20th Feb 1969

Educational Institutions Attended:

Anna University, Madras, India,1986-90.

Degrees Awarded:

B. E, Anna University, Madras, India, 1991.

Honours and Awards:

B. E, First class with distinction, Anna University, Madras, India, 1991.

Publications:

1. S. Subramanian, D. J. Shpak, P. S. R. Diniz, A. Antoniou, "The performance of adaptive filtering algorithms in a simulated HDSL environment," *Proc. Canadian Conf. Elec. and Comp. Eng.*, Toronto, pp. TA 2.19.1-TA2.19.4, Sept. 1992.

2. S. Subramanian, D. J. Shpak, A. Antoniou, "Adaptive equalization for HDSL," *IEEE Pacific Rim Conf. Comm., Comp., Signal Processing*, Victoria, May 1993.

3. S. Subramanian, D. Bhattacharya, D. J. Shpak, A. Antoniou, "Design of VLSI echo cancelers for HDSL systems," submitted to *Canadian. Conf. Elec. and Comp. Eng.*, Vancouver, Sept. 1993.

PARTIAL COPYRIGHT LICENSE

I hereby grant the right to lend my thesis to users of the University of Victoria Library, and to make single copies only for such users or in response to a request from the Library of any other university, or similar institution, on its behalf or for one of its users. I further agree that permission for extensive copying of this thesis for scholarly purposes may be granted by me or a member of the University designated by me. It is understood that copying or publication of this thesis for financial gain shall not be allowed without my written permission.

Title of Thesis: ECHO CANCELLATION AND EQUALIZATION FOR PRIMARY RATE ISDN SERVICE IN THE SUBSCRIBER LOOP PLANT

Author: [redacted]

(Signature)

SRIKANTH SUBRAMANIAN

(Name in Block Letters)

May 31, 1993

(Date)